Electrochemical properties and biomimetic activity of water-soluble *meso*-substituted Mn(III) porphyrin complexes in the electrocatalytic reduction of hydrogen peroxide.

Yulia G. Mourzina*, Andreas Offenhäusser

Institute of Complex Systems-8 (Bioelectronics), Forschungszentrum Jülich, 52425 Jülich, Germany and Jülich-Aachen Research Alliance (JARA) Fundamentals of Future Information Technology

* *Corresponding author: Dr. Yulia Mourzina, E-mail: y.mourzina@fz-juelich.de*

Abstract: The aim of this study was to investigate biomimetic activity of water-soluble manganese porphyrin complexes with a series of *meso*-substituents of the porphyrin macrocycle in the electrocatalytic reduction of hydrogen peroxide in aqueous solutions and to obtain information on possible intermediates, processes, and mechanisms. Mn porphyrins were compared in the process of the electrocatalytic reduction of hydrogen peroxide at pH 4, 7.4, and 10 in the deoxygenated solutions and in the presence of oxygen. The highest sensitivity, defined as the reduction current increase in relation to the concentration of hydrogen peroxide, was found in the case of Mn(III) *meso*-tetra(N-methyl-4-pyridyl) porphyrin, MnTMPyP, in alkaline $2.9 \cdot 10^{-2}$ A M^{-1} and acidic $1.6 \cdot 10^{-2}$ A M^{-1} solutions in the presence of oxygen. The reduction currents at pH 7.4, 10, and 4 in the presence of H_2O_2 were about 4, 7, and 12 times higher, respectively, in the solutions with the MnTMPyP complex than those at a GCE without a porphyrin complex in the solution. The electrocatalytic reduction of hydrogen peroxide occurs in parallel with an oxidative degradation of the porphyrin catalyst depending on the conditions of the experiment and was most significant in the presence of oxygen. The effect of the functional substituents at the *meso*-positions of a porphyrin ligand on the electrocatalytic activity of the water-soluble Mn(III) porphyrins complexes is discussed and reaction mechanisms are proposed.

Keywords: manganese porphyrin, electrocatalytic reduction, hydrogen peroxide, oxygen, biomimetic activity

1. Introduction.

Recently, there has been growing research interest in the detection of hydrogen peroxide and in understanding the mechanisms of the reactions with the participation of hydrogen peroxide because of the established role of hydrogen peroxide in biological signaling, oxidative stress conditions, and oxidative therapy [1, 2]. Moreover, hydrogen peroxide is attracting considerable attention in industrial and ecological applications, where it is a sustainable energy carrier in hydrogen peroxide fuel cells [3], an oxidant in catalytic epoxidation [4], organic pollutant degradation [5], and disinfection. Redox processes with the participation of hydrogen peroxide are often (electro)catalyzed by metal complexes.

In biological systems, iron, iron-copper, copper, and manganese active-site complexes mediate oxidation/oxygenation reactions using O_2 and H_2O_2 as the terminal oxidants reducing oxygen and hydrogen peroxide, respectively, while in a photosynthetic process a reverse process of water oxidation to oxygen takes place [6, 7]. There have already been studies of these biological processes in aqueous solutions, aimed at understanding the reaction mechanisms and intermediates of these biocatalytical transformations. In parallel, simpler metal complexes are being explored as biomimetic catalyst models to carry out oxidation/oxygenation reactions. Porphyrins were the ligands of choice to build the biomimetic metallocomplex catalysts in these studies because of their versatile role as biological ligands in nature, the possibility of fine tuning the environment of the central metal ion due to the electron withdrawing/donating and steric properties of the substituents of the porphyrin macrocycles, as well as the molecular association conditions. Most studies on the electrocatalysis of oxygen and hydrogen peroxide reduction with metal complexes of the N_4-macroheterocycles have been performed on iron, e.g. hemin, and cobalt complexes [7-16]. Accordingly, biomimetic binding and activation of the reduction of hydrogen peroxide are believed to have common metal-oxygen intermediates [7]. Investigations have been also performed with the metalloporphyrins and related compounds confined to the solid-state surfaces, with carbonaceous materials often being the materials of choice [9, 17-19]. However, the solid support can perform the role of an axial ligand affecting the properties of the metal center and, therefore, the reaction mechanisms of the metalloporphyrins in confined states and in liquid media could be different [9, 20].

Along with studies on the iron and cobalt complexes, there is growing research interest in the manganese N_4-macroheterocyclic complexes and in understanding their interactions with oxygen and hydrogen peroxide for their future utilization as active biomimetic components in a wide spectrum of (electro)catalytic systems in the fields of biology and therapy [7, 21-25], signaling, and oxidative stress conditions in plants [26] and higher organisms, chemistry [27], electroanalysis [18, 28-31], and sustainable energy research [32, 33]. Interest in the

investigation of the catalytic properties of manganese complexes is associated with their essential role in biological processes in the composition of manganese-containing catalases, in PS II, and also with the ability of the manganese ion to change its oxidation state from +2 to +7 [34]. Although there have been some investigations of the electrochemical properties of the manganese porphyrin complexes in organic media [7, 8, 35-38], or confined to the solid-state surface [17, 39], studies on their properties in aqueous media and the catalysis of electroreduction of dioxygen by manganese porphyrin complexes remain very limited [5, 40-50]. Moreover, the process of hydrogen peroxide electrocatalytic reduction is complicated by the oxygen reduction occurring simultaneously in the presence of oxygen and by the oxidation of Mn(III) complexes by hydrogen peroxide in solutions as in non-electrochemical conditions [34, 51].

The aim of this study is to investigate an electrocatalytic reduction process of hydrogen peroxide with water-soluble manganese porphyrin complexes with a series of meso-substituents of a porphyrin macrocycle and to obtain information on possible intermediates, processes, and mechanisms. The electrocatalytic reduction of hydrogen peroxide occurs simultaneously with a chemical interaction between hydrogen peroxide and manganese porphyrins. The interactions are investigated at physiological pH, since they are of importance for the development of *in vivo* and *in vitro* sensors as well as for enzyme mimic studies. The system is compared with acidic and alkaline media, where different products and mechanisms of chemical and electrochemical interactions are proposed and discussed.

2. Experimental

2.1. Reagents and solutions.

Mn(III) *meso*-tetra(4-carboxyphenyl) porphine chloride, Mn(III) *meso*-tetra(4-sulfonatophenyl)porphine chloride, Mn(III) *meso*-tetra(N-methyl-4-pyridyl) porphine pentachloride, Fig. 1a, with a purity of >95 % were obtained from Frontiers Scientific Inc., Utah, USA. Xanthine oxidase from bovine milk, cytochrome *c* from equine heart, and catalase were obtained from Sigma-Aldrich. All other chemicals were of analytical grade and supplied by Sigma-Aldrich Inc. All solutions were prepared using distilled water. Solutions of pH 4 were prepared by titrating the solutions of porphyrins in 0.1 M KNO_3 as a background electrolyte with HCl. 0.1 M phosphate buffer solution (PBS) of pH 7.4 was prepared from disodium hydrogen phosphate and sodium dihydrogen phosphate. Borate buffer solution of pH 10 was

prepared from sodium tetraborate decahydrate and sodium hydroxide with a background of 0.1 M potassium nitrate. The pH of the solutions was determined and adjusted using a laboratory pH meter.

2.2. Methods and apparatus.

Electrochemical characterization was performed with an Autolab PGSTAT100 potentiostat (Echo Chemie, the Netherlands), using an electrochemical cell with a three-electrode configuration. A double-junction Ag/AgCl electrode, Ag | AgCl | KCl 3 M::0.5 M KCl, (Metrohm, Switzerland), was used as a reference electrode. Pt coiled wire was used as an auxiliary electrode and a glassy carbon electrode (GCE) was the working electrode. An outer solution of the reference electrode was changed regularly after the measurements to prevent contamination of the electrode with porphyrins and the potential of the reference electrode was controlled with a Ag/AgCl (3 M) reference electrode (Sigma-Aldrich Inc.). GCEs with a diameter of 3 mm (a working geometrical area of 0.071 cm^2) were supplied by BASi Inc. Electroactive surface area of 0.064 cm^2 was found using a ferrocenemethanol redox couple [52]. The electrodes were treated before each measurement according to the procedure described in [33]. Deaeration of the solutions was accomplished by passing a constant stream of argon through the solution for 15 min before the experiment and maintaining a stream of argon over the solution during the experiment. The measurements were performed in triplicate.

Absorption spectroscopy was performed with a PerkinElmer Lambda 900 spectrometer. Quartz cuvettes with a path length of 1 mm or 5 mm (Sigma-Aldrich Inc.) were used.

2.3. Cytochrome c assay.

The assay was performed in a 3 ml of 0.05 M PBS, pH 7.8, in a cuvette with a path length of 1.0 cm [53]. The solution contained 10^{-4} M EDTA, 50 μM xanthine, 10 μM ferricytochrome *c*, and 15 μg ml^{-1} catalase to prevent the reoxidation of ferrocytochrome *c* by H_2O_2 produced in the reaction of the oxygen reduction catalyzed by xanthine oxidase. The reduction of ferricytochrome *c* was initiated by addition of xanthine oxidase. The amount of MnP complex, which inhibited the rate of reduction of cyt *c* by 50 %, IC_{50}, was found according to [54]. The rate constant for the reaction of $O_2^{\bullet -}$ with MnP was found by competition kinetics using cyt *c* as the reference [25, 55, 56]. Possible interference of the xanthine oxidase reaction

by MnP complexes was excluded by following the rate of accumulation of urate at 295 nm in the absence of cyt *c* [25].

3. Results and discussion.

3.1. Electrochemical and spectrophotometric characterization of the Mn(III) porphyrin complexes, Mn(III)TMPyP, Mn(III)TCPP, Mn(III)TSPP at pH 7.4, 10, and 4.

Ground-state absorption of manganese porphyrin complexes at pH 7.4 is shown in Figure 1b. The measured wavelength values, Table S1, are in a good agreement with the literature data [35, 57, 58] and were discussed in detail in [59]. A study of the dependence of the apparent molar absorptivity on the concentration for the manganese porphyrin complexes showed no evidence for an aggregation in a pH range of 4 to 10 and at the concentrations used except for Mn(III)TSPP and Mn(III)TCPP at pH 4, which is discussed in Section 3.5. The porphyrins were therefore considered to be monomers in all other conditions of the experiments. These results are consistent with previous reports [46].

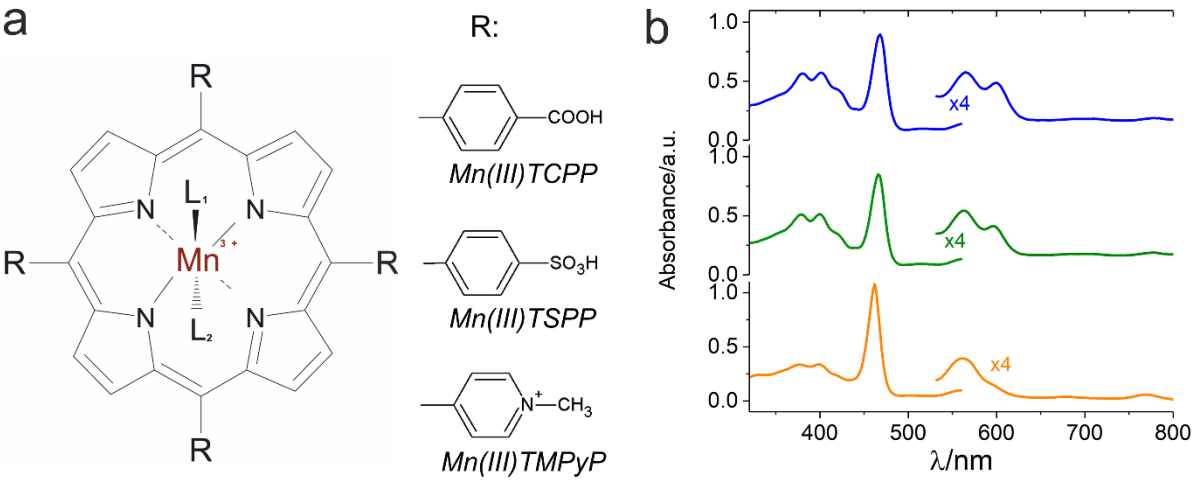

Fig. 1. a. The water-soluble Mn(III) *meso*-tetrasubstituted porphyrin complexes used. L_1 and L_2 may denote the aqua and hydroxo-ligand(s), whereat L_2 is not obligatorily present. **b.** UV-*vis* absorption of manganese porphyrin complexes: Mn(III)TCPP (blue line), Mn(III)TSPP (green line), and Mn(III)TMPyP (orange line). Other conditions: 0.1 M PBS, pH 7.4, porphyrin solutions of about $9 \cdot 10^{-5}$ M, room temperature, and cuvettes with a path length of 1 mm.

Examples of cyclic voltammograms of Mn(III)Ps obtained in deoxygenated aqueous buffer solutions of pH 7.4 are illustrated in Fig. 2 and S1a, and a summary of the data is given in Table 1. The curves in argon reveal peaks corresponding to the redox processes of the

conversion of the metal ion and porphyrin ligands. The first reduction wave at $E_p^{red.\ 1}$, Table 1, corresponds to a one-electron reduction of Mn(III) → Mn(II). The corresponding electrooxidation process Mn(II) → Mn(III) is observed in a reverse scan. This electroreduction process Mn(III) → Mn(II) is not displayed in CV performed in air, Fig. S1b,c due to the electrocatalytic activity of the metalloporphyrins for the oxygen reduction reaction (ORR), which is higher for the MnTMPyP complex as will be discussed below. The second reduction wave in the case of MnTMPyP in the deoxygenated solution appears at -0.77 V (pH 7.4) and can be assigned to the electrochemical reduction of the porphyrin ligand to the porphyrin π-radical anion (one-electron reduction) or dianion (two-electron reduction). In the case of MnTCPP and MnTSPP, the second reduction does not occur at the potential window investigated. More positive values of the Mn(III/II) and porphyrin ligand reduction, Fig. 2, as well as porphyrin ligand oxidation, Fig. 2 and Table 1, in the case of MnTMPyP may be explained taking into account the electron-withdrawing nature of the N-methyl-4-pyridyl substituent in comparison with 4-sulfonatophenyl- and 4-carboxyphenyl substituents [33, 60]. Similar electrochemical behavior was observed at pH 10 and 4, as is shown below.

We assume that the oxidation process at electrochemical potential values between 0.8 V and 0.9 V, Fig. 2, belongs to the oxidation of Mn(III)P to Mn(IV)P (0.898 V for MnTCPP, 0.889 V for MnTSPP, and 0.830 V for MnTMPyP), which is a quasi-reversible process in the case of the MnTMPyP complex under the conditions of experiment. Electrochemical reduction of $Mn^{IV/III}$ was not observed for the MnTCPP and MnTSPP complexes under the conditions of experiment, which might be due to kinetic and thermodynamic limitations associated with acid-base equilibria of axially coordinated water molecules [61] or subsequent Mn(IV) complex decomposition by chemical reaction [50], as well as properties of the irreversibly oxidized porphyrin ligand in those cases and requires further investigations. These observations find an agreement with previous studies [47, 48, 50, 58], where the Mn(IV/III)P redox couple of the complex was observed only in alkaline solutions. In the study of A. Harriman [61], $Mn^{III/IV}P$ oxidation approached the fully reversible case at pH >13 but as the pH dropped below 12.5 the redox wave became difficult to resolve.

Table 1. Electrochemical characterization of the Mn(III) porphyrin complexes in a phosphate buffer solution at pH 7.4.

	$E_p^{red.\ 1}$/ V	$E_p^{ox.\ 1}$/ V	$\Delta E^{\ 1}$/ mV	$k_{et}\cdot 10^{3\ 3}$/ cm s^{-1}	$E_p^{L\ red.\ 2}$/ V	$E_p^{L\ ox.\ 4}$ /V	$E(O_{2\ red.})$ with MnP

	Mn(III/II)						
MnTCPP	-0.503	-0.421	82	1.7±0.2	<-1.2	1.061	-0.540 (0.1) [5]
MnTSPP	-0.480	-0.393	87	1.2±0.1	<-1.2	1.108	-0.611 (0.03) [5]
MnTMPyP	-0.228	-0.156	72	9.6±0.8	-0.77	>1.2	-0.433 (0.21) [5]

[1] - $E_p^{red.}$, $E_p^{ox.}$, and ΔE of the Mn(III/II) redox process in a deaerated solution and at a scan rate of 0.005 V s^{-1}.

[2] - $E_p^{L\ red.}$ for the reduction of the porphyrin ligand ($L_{red.}$).

[3] - found using the Nicholson method and a diffusion coefficient value of $2.12 \cdot 10^{-6}$ cm^2 s^{-1}, n=3.

[4] - $E_p^{Lox.}$ for the one- or two-electron oxidations of the porphyrin ligand, scan rate 0.05 V s^{-1}.

[5] - positive shift of the potential of oxygen reduction in comparison with that of oxygen reduction at a GCE without a porphyrin complex in solution is given in the brackets.

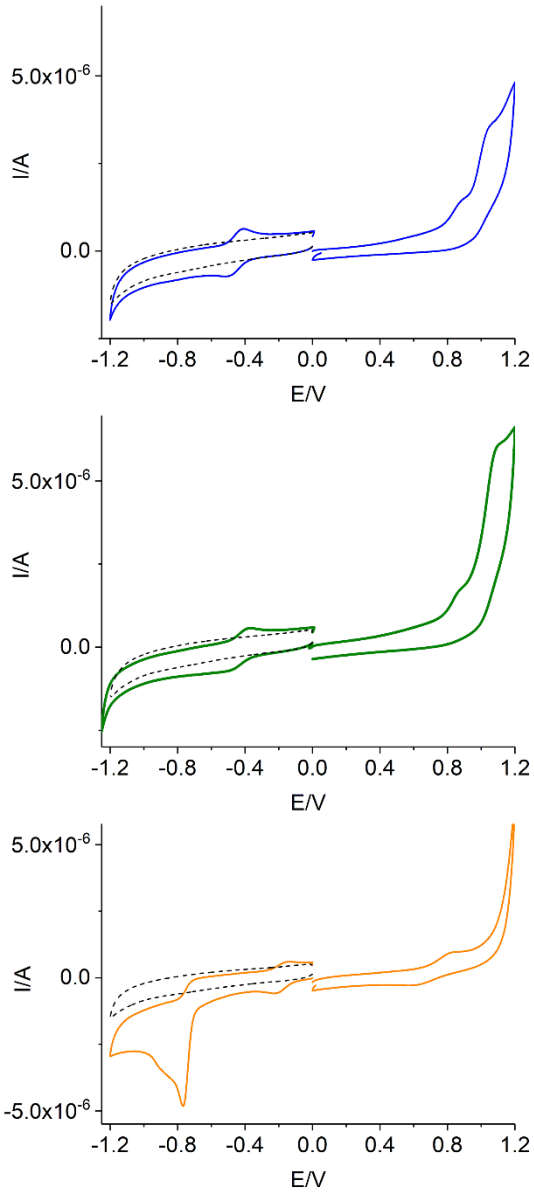

Fig. 2. Cyclic voltammograms of the manganese (III) porphyrin complexes in a deoxygenated 0.1 M PBS, pH 7.4, GCE: Mn(III)TCPP (blue line), Mn(III)TSPP (green line), Mn(III)TMPyP (orange line), GCE in PBS without Mn porphyrin complexes (black dotted lines), scan rate 0.05 V s^{-1}.

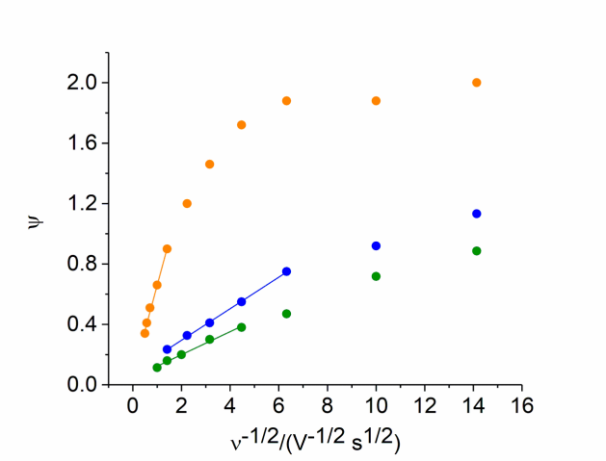

Fig. 3. Plot of the kinetic parameter, ψ, *versus* the reciprocal of the square root of the scan rate, $\upsilon^{1/2}$ [62], for the $Mn^{III/II}$ redox processes in a deoxygenated PBS, pH 7.4: Mn(III)TCPP (blue circles), Mn(III)TSPP (green circles), Mn(III)TMPyP (orange circles), and the corresponding linear fit curves with R^2=0.9991, R^2=0.9909, and R^2=0.9900, respectively.

Fig. S1a demonstrates a linear dependence of the Mn(III)/Mn(II) peak currents on a square root of the scan rate, a I_p - $\upsilon^{1/2}$ dependence, with good correlation coefficients, characteristic of a diffusion-controlled redox process. A similar dependence was obtained for Mn(III)TCPP and Mn(III)TSPP porphyrin complexes. Fig. 3 shows that the peak-to-peak separation, ΔE_p, of the quasi-reversible electrochemical $Mn^{III/II}$P reactions increases with the scan rate, which allows the heterogeneous rate constants of the electron transfer for the $Mn^{III/II}$ redox processes to be determined by the Nicholson method [62]:

$$\psi = k_s (D_O/D_R)^{\alpha/2} / (\pi D_O n F \upsilon/RT)^{1/2} \qquad (1),$$

where ψ is a dimensionless kinetic parameter determined from ΔE_p of the quasi-reversible electrochemical reaction [62], k_s is a heterogeneous rate constant of the redox reaction (cm s^{-1}), D_O and D_R are diffusion coefficients of the oxidized and reduced form (cm^2 s^{-1}), respectively, n is the number of electrons transferred in the reaction, F is the Faraday constant (96485 V mol^{-1}), R is the gas constant (8.3145 J $mo1^{-1}$ K^{-1}), and T is the temperature (K). Except for unusual cases, the quantity $(D_O/D_R)^{\alpha/2}$ is very close to unity. As expected from the Nicholson equation (1), the dimensionless kinetic parameter determined from ΔE_p of the quasi-reversible electrochemical reaction shows a theoretically predicted linear dependence versus the reciprocal of the square root of the scan rate in a useful scan range interval for the $Mn^{III/II}$P redox processes, Fig. 3. A deviation from linearity in the case of MnTMPyP at low scan rates is due to approaching the reversibility of the $Mn^{III/II}$TMPyP electrode reaction and a diffusion-controlled redox process at low scan rates, when ΔE_p approaches a theoretical value of 59 mV,

Fig. S1a and 3. Therefore this interval of scan rates was not considered for the determination of the electron transfer rate constant of $Mn^{III/II}$TMPyP using the Nicholson method and Eq. (1).

Diffusion coefficients of the Mn(III)P used in Eq. (1) were found from the Randles-Sevcik equation:

$$I_p = 0.446\left(\frac{n^3F^3D\upsilon}{RT}\right)^{1/2}Ac \qquad (2).$$

Although Eq. (2) is widely used to determine the diffusion coefficients, it is valid for the reversible electrochemical reaction, where the mass-transport component is rate-limiting. Therefore, we used the Randles-Sevcik equation to evaluate the diffusion coefficient of MnTMPyP at a low scan rate of 0.005 V s^{-1}, where the peak separation of 0.072 V is closest to the theoretically expected value for the reversible redox reaction value of 0.059 V. The diffusion coefficient of MnTMPyP was found to be $2.12\cdot10^{-6}$ cm^2 s^{-1}. This value is close to the values of the diffusion coefficients found for the water-soluble Mn(III) *ortho* and *meta* substituted N-ethylpyridyl porphyrins in aqueous solutions at pH 7.5 of $2.35\cdot10^{-6}$ cm^2 s^{-1} and $2.15\cdot10^{-6}$ cm^2 s^{-1} [47], respectively. The heterogeneous electron transfer rate constants found for the electrochemical redox reaction of the Mn(III/II) porphyrin complexes from the slope of the lines fitted to the experimental data points in Fig. 3 using a diffusion coefficient value of $2.12\cdot10^{-6}$ cm^2 s^{-1} are listed in Table 1. The k_s(MnTMPyP) is about 5.8 to 8 times higher than the corresponding values of k_s(MnTCPP) and k_s(MnTSPP), respectively. Altogether, the details of the cyclic voltammetry experiments demonstrate more positive potential values and faster electron transfer kinetics of the $Mn^{III/II}$P redox process for the MnTMPyP complex in comparison with MnTCPP and MnTSPP complexes at neutral pH, Fig. 2 and Table 1. The former may be explained by modulating the redox potentials of the porphyrin complexes by using an electron-withdrawing substituent on the porphyrin macrocycle, which is in agreement with the stronger electron-withdrawing character of the N-methyl-4-pyridyl substituent groups. The faster electron transfer kinetics may be explained by the positively charged and less bulky N-methyl-4-pyridyl groups in comparison with 4-carboxyphenyl and 4-sulfonatophenyl groups, which facilitates a closer approach of the MnMPyP to the negatively charged electrode surface for the redox process.

Similar tendencies were observed in the alkaline and acidic solutions at pH 10, Fig. 4, S2, Table 2, and pH 4, Fig. 5 and Table 3, respectively. In general, electrochemical experiments showed no essential pH dependence of the formal reduction potential of the Mn^{III}P/Mn^{II}P redox couples in the pH range studied, which is in agreement with previous reports, where the formal reduction potential of the Mn^{III}P/Mn^{II}P redox couple of the MnTMPyP complex was pH-independent in a pH range of about 3 to 10 [45, 47]. The observed small shift of the

electrochemical potential for manganese reduction can be related to the changes of the protonation state of water molecule(s) coordinated at the axial positions [22, 24, 47, 49].

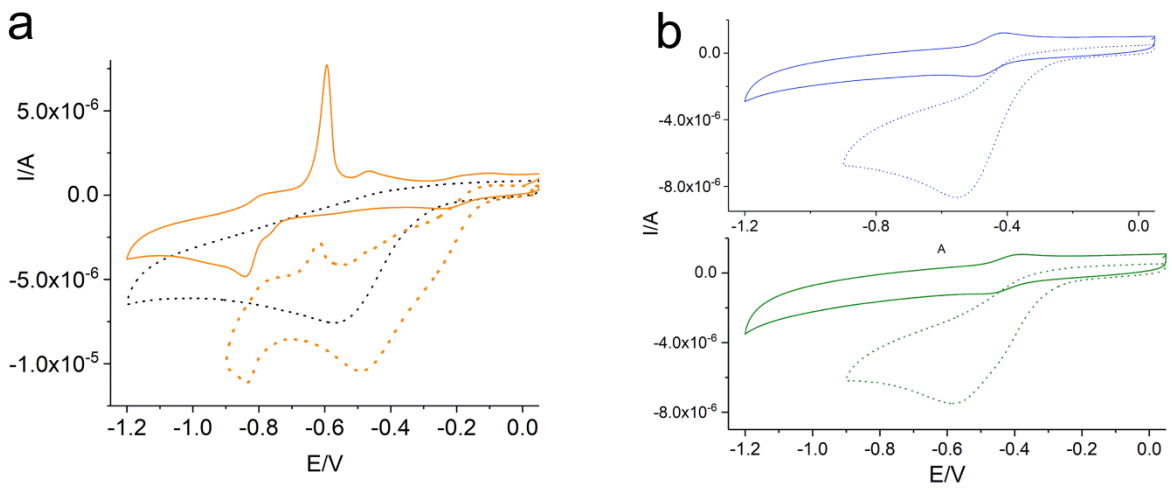

Fig. 4. Cyclic voltammograms of the manganese (III) porphyrin complexes in a borate buffer of pH 10: Mn(III)TCPP (blue line), Mn(III)TSPP (green line), Mn(III)TMPyP (orange line), solid lines - in a deoxygenated buffer, dotted lines - in the presence of oxygen. In part **a**, a dotted black line shows a cyclic voltammogram of a GCE in the absence of a Mn(III) complex and in the presence of oxygen, scan rate 0.05 V s^{-1}, GCE**.**

Table 2. Electrochemical characteristics of the Mn(III) porphyrin complexes in an alkaline buffer, pH 10.

	$Mn^{III/II}$			$E_p^{L\ red.\ 2}$/ V	$E_p^{L\ ox.\ 2}$/ V
	$E_p^{red.\ 1}$/ V	$E_p^{ox.\ 1}$/ V	ΔE^{1}/ mV		
MnTCPP	-0.497	-0.414	83	<-1.2	1.063
MnTSPP	-0.481	-0.384	97	<-1.2	1.102
MnTMPyP	-0.232	-0.161	71	-0.84	>1.2

[1] - $E_p^{red.}$, $E_p^{ox.}$, and ΔE of the Mn(III/II) redox process in a deoxygenated solution.
[2] - $E_p^{L\ red.}$ for the reduction of the porphyrin ligand and $E_p^{Lox.}$ for the oxidation of the porphyrin ligand in deoxygenated solutions.

However, the reduction of the TMPyP ligand of the MnTMPyP complex at pH 10 occurs at more negative potential values in comparison with neutral pH, Tables 1 and 2, and Figs. 2 and 4a, while in the acidic solutions the reduction of the TMPyP and TSPP ligands occurs at more positive potential values, Table 1 and 3, and Figs. 2 and 5a. The electrochemical reduction of the porphyrin ligand in the MnTMPyP complex takes place at more positive potentials in acidic solution, demonstrating a pH dependence of 22 - 27 mV/dec in the studied pH range of 4 to 10. Similarly, the electrochemical reduction of the porphyrin ligand in the MnTSPP

complex can be observed only in acidic solutions. These electrochemical properties may be explained by the availability of hydrogen ions in the acidic media, since the reduction of porphyrin ligands is accompanied by their protonation [63, 64], so that the porphyrin ligands of the MnTMPyP and MnTSPP complexes are more easily reduced in acidic media.

Additionally, a sharp peak of the anodic current is observed in the case of MnTMPyP in a reverse scan at pH 10, which is probably related to the oxidative adsorption process of a porphyrin. Similar to the neutral buffer, MnTMPyP demonstrated the highest electrocatalytic activity for the oxygen reduction process, as follows from a comparison of Figs. 4a and b as well as Fig. 5b, which will be discussed in Sections 3.2 and S1.

Solution pH (in the studied pH range of 4 to 10) does not influence the λ_{max} of the UV-vis spectra essentially, as can be seen from Tables S1-S3. These results are in agreement with a previous report, where no changes in the UV-vis spectra between pH 2 and attaining the first pK_a value of 10.5 of Mn(III) complex were reported [46].

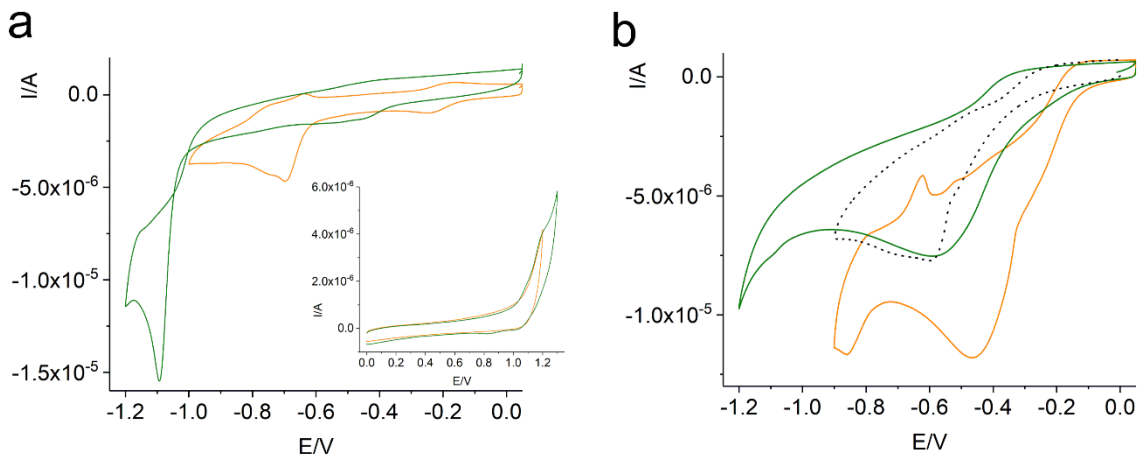

Fig. 5. Cyclic voltammograms of the manganese (III) porphyrin complexes at pH 4: Mn(III)TSPP (green line) and Mn(III)TMPyP (orange line): **a.** deoxygenated, **b.** in the presence of oxygen, dotted black line corresponds to the CV of a GCE without a porphyrin complex in the solution; scan rate 0.05 V s^{-1}. Mn(III)TCPP is insoluble at the same conditions.

Table 3. Electrochemical characteristics of the Mn(III) porphyrin complexes at pH 4 [1].

	Mn III / II		E_p L red. [3]/ V	E_p L ox. [3]/ V
	E_p red. [2]/ V	E_p ox. [2]/ V		
MnTSPP	-0.496	-0.400	-1.093	1.19
MnTMPyP	-0.243	-0.172	-0.697	>1.2

[1] - MnTCPP is insoluble at pH 4.
[2] - $E_p^{red.}$, $E_p^{ox.}$ of the Mn(III/II) redox process in a deaerated solution.

[3] - $E_p^{L\ red.}$ for the reduction of the porphyrin ligand and $E_p^{L\ ox.}$ for the oxidation of the porphyrin ligand in the deoxygenated solutions.

3.2. Electrochemical behavior of the water-soluble Mn(III) porphyrin complexes in the presence of the oxygen reduction reaction.

Since in most cases the electrochemical reduction of hydrogen peroxide is considered in the presence of oxygen, the electrochemical behavior of the Mn(III) porphyrin complexes was investigated in corresponding conditions. The cyclic voltammograms of the Mn(III)P complexes in the electrolyte in the presence of oxygen, Fig. S1b,c, display changes in the potential range where the ORR occurs compared to the CVs in the deoxygenated solutions, Fig. 2. In the presence of oxygen, no wave of the Mn(III)/Mn(II) reduction is observed in the cathodic region even for the more electronegative MnTMPyP at all pH studied. The reduction of Mn(III) and O_2 merges with a positive shift of the O_2 reduction of about 0.21 V for Mn(III)TMPyP and 0.1 V for Mn(III)TCPP at pH 7.4, Fig. S1b,c, Table 1, and Section S1.

According to the results of the experiments, the Mn porphyrin complexes used in the study act as electrocatalysts decreasing the overpotential of the oxygen reduction reaction on a GCE and increasing the reduction currents due to the involvement of a metal in the process of the oxygen reduction reaction, which agrees with previous investigations [16, 25, 41, 45-48, 50], Section S1. In most cases, a significant increase of the reduction current was observed at all three pH studied, which may be explained by an electrocatalytic reduction of oxygen and redox cycle according to a tentative Scheme 1 for the pH used [8, 45, 46, 65, 66].

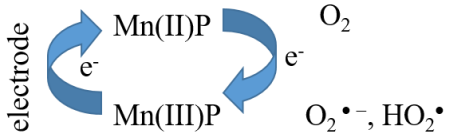

$$Mn(III)TMPyP^{5+} + e^- \rightarrow Mn(II)TMPyP^{4+}$$

$$Mn(II)TMPyP^{4+} + O_2 \rightarrow Mn(III)TMPyP^{5+} + O_2^{\bullet -}$$

Scheme 1. Scheme of a catalytic oxygen reduction promoted by the MnP complex (left) and a model for the outer-sphere catalysis involving a superoxide anion radical or a less common – hydroperoxyl radical as the initial species of the oxygen reduction, pKa($HO_2^{\bullet}$)=4.7 [67].

3.3. Electrocatalytic reduction of hydrogen peroxide with Mn porphyrin complexes, pH 7.4.

As in the case of oxygen reduction, the electrocatalytic reduction of hydrogen peroxide starts at potentials where a Mn(III)/Mn(II) reduction process takes place, Fig. 6 and S3. As

summarized in Fig. 7 and Table 4, the current response to the changes of the H_2O_2 concentration increases for all three porphyrins in comparison to that of a bare GCE in a phosphate buffer both in the absence of oxygen and in air, with the current response being more pronounced in the aerated buffer. For example, the electroreduction current at -0.44 V in the presence of $4 \cdot 10^{-3}$ M H_2O_2, Fig. 7b, was about 4 times higher in the presence of the MnTMPyP complex. MnTMPyP demonstrates the highest electrocatalytic activity at lower potential values, while the MnTCPP and MnTSPP complexes behave similarly, Fig. 7.

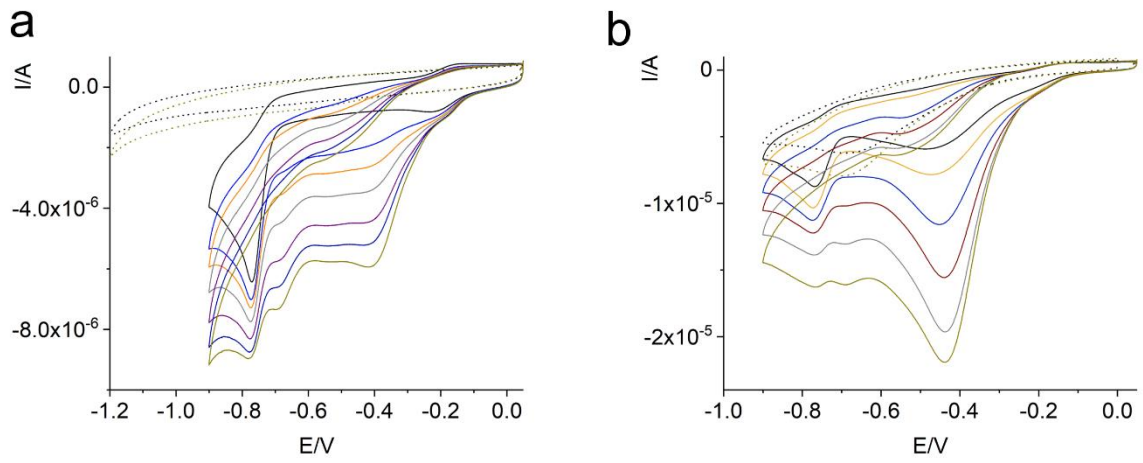

Fig. 6. Cyclic voltammograms of Mn(III)TMPyP complex in a phosphate buffer solution, pH 7.4: **a.** - deoxygenated buffer, dotted lines - in the absence of the Mn(III)TMPyP complex, solid lines - in the presence of Mn(III)TMPyP complex, H_2O_2 from 0 M (black lines) to $3.9 \cdot 10^{-3}$ M (dark yellow lines), **b.** - in the presence of oxygen, dotted lines show CVs in the absence of Mn(III) porphyrin complex, H_2O_2 from 0 M (black lines) to $3.4 \cdot 10^{-3}$ M (dark yellow lines). Other conditions: $9 \cdot 10^{-5}$ M MnTMPyP, scan rate 0.05 V s^{-1}.

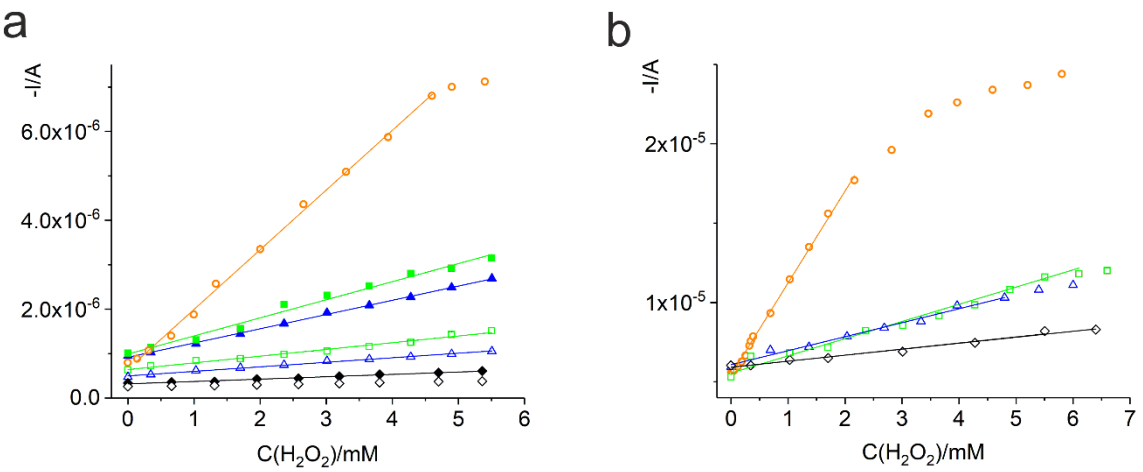

Figure 7. Dependence of the reduction current on the concentration of hydrogen peroxide in a phosphate buffer, pH 7.4, with $9 \cdot 10^{-5}$ M porphyrin complexes: MnTMPyP - orange circles,

MnTCPP - blue triangles, MnTSPP - green squares, and a bare GCE - black diamonds; **a.** - deoxygenated buffer, open symbols - current at -0.4 V, closed symbols – current at -0.5 V, **b.** - in the presence of oxygen, -I at -0.57 V are given for MnTCPP, MnTSPP, and a bare GCE, and -I at -0.44 V are given for MnTMPyP. Scan rate 0.05 V s^{-1}.

Table 4. Slope and correlation coefficients of the -I-c(H_2O_2) curves in a phosphate buffer solution, pH 7.4.

	deoxygenated PBS, pH 7.4 [1]		PBS, pH 7.4 [1]	
	b	R^2	b	R^2
MnTCPP	$3.2 \cdot 10^{-4}$ (E=-0.5 V)	0.99862	$8.8 \cdot 10^{-4}$ (E=-0.57 V)	0.9826
MnTSPP	$4.1 \cdot 10^{-4}$ (E=-0.5 V)	0.98491	$1.1 \cdot 10^{-3}$ (E=-0.57 V)	0.9742
MnTMPyP	$1.4 \cdot 10^{-3}$ (E=-0.4 V)	0.99692	$5.8 \cdot 10^{-3}$ (E=-0.44 V)	0.9977
GCE	$5.3 \cdot 10^{-5}$ (E=-0.5 V)	0.98671	$3.8 \cdot 10^{-4}$ (E=-0.57 V)	0.9814

[1] In brackets, potential values are given at which reduction current values for the -I-c(H_2O_2) curves were used to evaluate b and R^2 parameters given in the table.

A comparative analysis of cyclic voltammograms in Fig. 6a,b and S3 shows that the electrochemical features of the reaction of the Mn(III)P complexes with hydrogen peroxide are different in the absence and presence of oxygen.

For comparison, Fig. S4a shows cyclic voltammograms at a bare GCE in the corresponding buffer solution. The reduction of hydrogen peroxide at the GCE proceeds at slightly more negative potentials of about -0.69 V than the potential at which the reduction of oxygen occurs, which is in agreement with a previous study [15, 68]. Two processes practically overlap in the potential region of -0.65 V to -0.69 V [15]. Accordingly, the MnTMPyP complex decreases the reduction overpotential of not only O_2 but also H_2O_2 by approx. 210 to 290 mV at pH 7.4 and increases the reduction currents as follows from a comparison of Figures 6, 7, S4a, and Table 4 for the deoxygenated buffer and in the presence of oxygen, respectively. Similar conclusions can be drawn for the MnTCPP and MnTSPP complexes, Figs. 7, S3, S4a, and Table 4. The electrocatalytic effect is highest for the MnTMPyP, while Mn(III)TCPP and Mn(III)TSPP have similar effects, as was also the case for the oxygen reduction discussed in Section 3.2 and section S1.

The onset of the hydrogen peroxide reduction process coincides with an onset of Mn(III)/Mn(II) reduction in both deoxygenated systems and in the presence of oxygen. In the latter system, the hydrogen peroxide reduction is displayed in a serial increase of the reduction currents according to the increasing concentrations of H_2O_2, Fig. 6b in comparison with the oxygen reduction in the absence of hydrogen peroxide, Fig. 6b (black solid line at C(H_2O_2)=0

M). This indicates an involvement of a metal-reduced form of the porphyrin in the electrocatalytic reduction of hydrogen peroxide similar to the electrocatalytic reduction of oxygen and agrees with the discussion above.

The initial two-electron reduction of the porphyrin ligand of the Mn(III)TMPyP in the absence of hydrogen peroxide at about -0.77 V, Fig. 2 and Table 1, proceeds via two one-electron reduction steps in the presence of hydrogen peroxide in both systems (in the presence and absence of oxygen), Fig. 6a,b, with the appearance of the first one-electron oxidation at about -0.690 V in both systems and the second electron reduction at -0.777 and -0.763 V, Scheme 2. This transfer may be explained by a change in the axial ligation and protonation steps in the course of the reaction with oxygen species, which influences the redox behavior of the complex [51, 63].

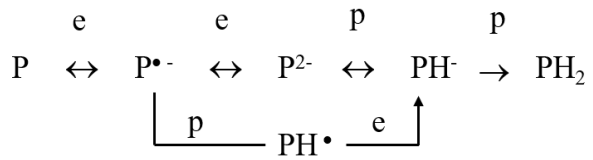

Scheme 2. Scheme of the reduction process for the porphyrin ligand, where e is a 1-e electron transfer process and p is a single protonation process [33].

From a comparison of Figs. 6 a and b, it can also be seen that in both systems the reduction current reaches its maximum at the close potential values of about -0.4 V (deoxygenated at -0.41 V and in the presence of air at -0.44 V). However, it is of interest that the reduction current in the deoxygenated solution does not decrease as in Fig. 6b forming a peak as in normal CV, but forms a plateau of the reduction current at a voltage interval of about -0.4 to -0.6 V. This indicates a permanent generation or presence of the species which are reduced at this potential window. The nature of these species is currently not clear, but reflects different mechanisms and intermediate species produced in the deoxygenated solution and in the presence of oxygen. After about -0.6 V, the reduction of the porphyrin ligand starts in both systems. The difference in a potential interval of -0.4 V to -0.6 V may be explained as follows. In the absence of oxygen, all generated metal-reduced forms of porphyrin, Mn(II)P, near the electrode surface are involved in the reaction with hydrogen peroxide according to the tentative reaction schemes described by Eqs. (1) – (5) or (6) – (10) for different pH ranges and based on previous investigations of the reactivity of MnP complexes implying the O-O bond dissociation [6-8, 13, 15, 24, 36, 44, 51], thus producing a plateau of the reduction current due to the catalytic

redox cycling in this potential range (porphyrin charges as well as L_1 and L_2, which might be aqua or hydroxo ligand(s) are omitted in the equations):

$$Mn(III)P + e^- \rightarrow Mn(II)P \quad (1)$$

$$Mn(II)P + H_2O_2 \rightarrow (H_2O_2)Mn(II)P \quad (2)$$

$$(H_2O_2)Mn(II)P \rightarrow (O^{\bullet})Mn(III)P + H_2O \quad (3)$$

$$(O^{\bullet})Mn(III)P \xrightarrow{e^-,\ H^+\ (H_2O)} (OH)Mn(III)P\ (+OH^-) \quad (4)$$

$$(OH)Mn(III)P + H^+\ (H_2O) \rightarrow Mn(III)P + H_2O\ (OH^-) \quad (5)$$

$$Mn(III)P + e^- \rightarrow Mn(II)P \quad (6)$$

$$Mn(II)P + H_2O_2 \rightarrow (H_2O_2)Mn(II)P \xrightarrow[-H^+]{} (HOO)Mn(II)P\ (\text{hydroperoxo}) \quad (7)$$

$$(HOO)Mn(II)P \xrightarrow{+H^+} O{=}Mn(IV)P\ /\ O{=}Mn(III)P^{\bullet +} + H_2O \quad (8)$$

$$O{=}Mn(IV)P\ /\ O{=}Mn(III)P^{\bullet +} \xrightarrow{e^-,\ H^+\ (H_2O)} (OH)Mn(III)P + (OH^-) \quad (9)$$

$$(OH)Mn(III)P + H^+\ (H_2O) \rightarrow Mn(III)P + H_2O\ (OH^-) \quad (10)$$

In the presence of oxygen, Fig. 6b, a plateau of the reduction current is not observed. This can be explained by the fact that a reduced Mn(II)P is consumed in the parallel reaction of oxygen reduction as in Scheme 1 disturbing the catalytic redox cycle in Eqs. (1-5) or (6-10) so that the electrochemical reaction is then mass-transport limited by a diffusion of MnTMPyP to the electrode surface. Moreover, taking into account the fact that an initial product of the oxygen reduction is a superoxide anion radical, reduction of Mn(III)P and oxidation of Mn(II)P by the superoxide in solutions are other possible parallel chemical reactions in the presence of oxygen due to the superoxide dismutase mimicking activity established for the Mn porphyrin complexes [55], Scheme 3:

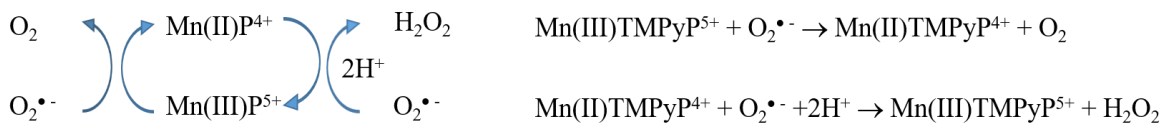

Scheme 3. Scheme of the superoxide dismutase-like activity of the MnTMPyP complex.

We examined the superoxide dismutase mimicking activity using the cytochrome *c* reduction assay by the xanthine-xanthine oxidase system [25, 53, 55], section 2.3 and Fig. S5. Rate constants for the reaction of the metalloporphyrin complex with $O_2^{\bullet -}$ can be evaluated

based on its competition with ferricytochrome *c* for reaction with $O_2^{\bullet -}$ using $k_{O2\bullet -,\ cyt\ c(3+)}=3\cdot10^6$ M^{-1} s^{-1} [55]. As one can see from Fig. S5, the MnTCPP and MnTSPP complexes were negligibly active in the assay conditions in comparison with MnTMPyP. Using the evaluation of Sawada and Yamazaki [54], we found the amount of MnTMPyP required to inhibit the rate of reduction of ferricytochrome *c* by 50 % IC_{50}(MnTMPyP)=(0.84±0.08) μM and the rate constant for the reaction of Mn(III)TMPyP with $O_2^{\bullet -}$ of $3.6\cdot10^7$ M^{-1} s^{-1}. Thus, on the one hand, presence of oxygen results in the consumption of the electroreduced catalytically active Mn(II)P, which would otherwise reduce hydrogen peroxide. On the other hand, the produced superoxide may chemically reduce Mn(III)P in the solution to the active Mn(II)P form. However, the superoxide dismutase mimicking activity of MnTMPyP may nevertheless diminish the reduced form Mn(II)P, which is available for the electrocatalytic reduction of hydrogen peroxide, since the oxidation of Mn(II) with $O_2^{\bullet -}$ is faster than the reduction of Mn(III) with $O_2^{\bullet -}$, i.e. the upper equation in Scheme 3 is a rate-limiting step [25, 55]. At present, it is difficult to distinguish the role of individual processes in the general reaction mechanism and kinetics, for which further studies should be undertaken.

It is also of interest that the reduction currents are higher in the presence of oxygen than in the deoxygenated buffer in the same concentration ranges of hydrogen peroxide. In the presence of the oxygen reduction reaction, as in Scheme 1, superoxide anion radical, $O_2^{\bullet -}$, may promote an oxidative cleavage of the O-O bond of hydrogen peroxide axially ligated to a reduced Mn(II) porphyrin complex with hydrogen atom transfer (HAT, $H^+ + e^-$) to $O_2^{\bullet -}$, transforming the superoxide anion radical into a 2e-reduced dioxygen, ^-O_2H, with the formation of high-valent Mn-oxo complexes and a radical cation on a porphyrin ring [6, 7, 44, 69], as in Scheme 4. In a recent study [22], the formation of the oxomanganyl π-radical cation $[(O=)Mn^{IV}P]^{\bullet +}$, a manganese analog of Compound I of heme peroxidases, in a chemical reaction of a manganese porphyrin incorporated into the protein scaffold with hydrogen peroxide was observed. The authors excluded the formation of the detectable $[(O=)Mn^{V}P]$. The formation of high-valent porphyrinate models including also six-coordinate complexes was extensively studied by J.T. Groves and co-workers and high-valent oxo-complexes $(O)Mn^{IV}P$, $(O)(H_2O)Mn^{V}P$, and $(O)_2Mn^{V}P$ were also discussed for a number of porphyrin complexes under different conditions of chemical oxidation [44, 70, 71]. Thus, as a result of the synergic electrocatalytic effect of MnP and oxygen, additional amounts of hydrogen peroxide may be produced near the electrode surface thus supplementing the amounts of hydrogen peroxide initially present in the solution, generating higher reduction currents. Moreover, due to competition with hydrogen peroxide for the reduction equivalents from the reduced Mn(II)P

complex, the superoxide anion may undergo dismutation (either spontaneously or catalyzed by MnP [55]):

$2O_2^{\bullet -} + 2H^+ = O_2 + H_2O_2$ (11).

This contribution to the overall process would also result in the higher reduction currents. However, a low catalase activity of the water-soluble Mn porphyrins was reported [21, 72] but rather an oxidative degradation of Mn porphyrins in the presence of H_2O_2, which was also observed in our spectrophotometric experiments as shown below. On the other hand, a catalase activity of Mn(III)TPPS in a basic aqueous hydrogen peroxide medium was observed [71].

Hence, a number of the tentative pathways are indicated in the text and summarized in Schemes 1,3,4, and Eqs. (1-11) and further studies may be necessary to elucidate a contribution of a particular reaction into an overall process of electrocatalytic reduction of hydrogen peroxide in different conditions. The high-valent Mn-oxo complexes or π-radical cation, as e.g. in eqn. (8), which are formed in the process, are not reversibly reduced, which results in a faster degradation of the MnP catalyst. Altogether, this "oxygen-reach" system, Figs. 6b and S3b,d, demonstrates a higher oxidation capacity, which is evident from the higher reduction currents (consumed electrons) and faster degradation of the porphyrin as discussed below.

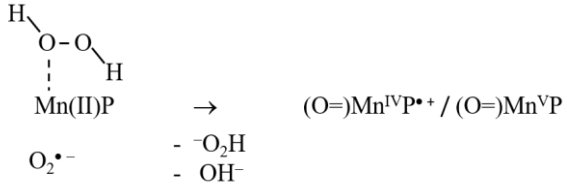

Scheme 4. A tentative scheme of an electrocatalytic process with participation of hydrogen peroxide and superoxide anion.

As can be seen from Figure 7, a linear dependence of the reduction peak currents on the concentration of hydrogen peroxide for the MnTMPyP complex is linear up to higher concentrations of H_2O_2 for the deoxygenated solutions (up to about a 60-fold excess of the hydrogen peroxide concentration) than that in the presence of oxygen (up to about a 24-fold excess of the hydrogen peroxide concentration). This may indicate a faster degradation of a porphyrin complex in the conjunct presence of hydrogen peroxide and oxygen than in a deoxygenated atmosphere. This is confirmed by absorption spectroscopy of the reaction products.

As can be concluded according to curves 1-3 in Fig. 8a, MnTMPyP is still present in the solution after the cathodic reaction with H_2O_2 in a deoxygenated buffer according to its characteristic absorption at 462 nm, while no porphyrin is present after electrochemical

experiments in the presence of oxygen, curve 4. Absorption at 462 nm, curves 1 and 2, decreases after the initially deoxygenated solution comes into contact with oxygen (air), which is noticeable in the consecutive measurements 1 to 3 in the presence of oxygen. The final curve 3 practically coincides with the absorbance of the solution after electrochemical experiments in the presence of oxygen, curve 4. Thus, faster degradation of a porphyrin takes place during electrochemical reaction in the conjunct presence of hydrogen peroxide and oxygen than in a deoxygenated atmosphere.

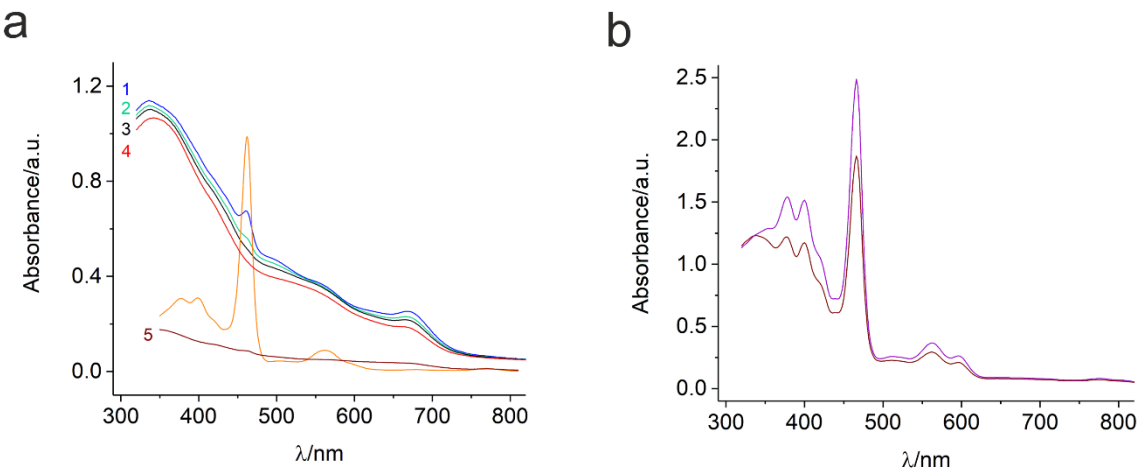

Fig. 8. UV-vis absorption in PBS, pH 7.4: **a.** consecutive spectrophotometric measurements of the MnTMPyP solution after electrochemical experiments with H_2O_2 in a deoxygenated buffer solution in the sequence 1 - *blue*, 2 - *green*, and 3 - *black lines*, spectrophotometric measurements of the MnTMPyP solution after electrochemical experiments with H_2O_2 in the presence of oxygen - *red line 4*, ground-state absorption spectrum of the Mn(III)TMPyP complex - *orange line* - is given for comparison, and absorption of the MnTMPyP solution in the presence of a large excess of H_2O_2 (1:1000) - *brown line 5;* **b.** spectrophotometric measurements of the Mn(III)TSPP solutions after electrochemical experiments (as in Fig. S3) in the deoxygenated buffer solution (*violett line*) and in the presence of air (*brown line*).

After electrochemical experiments with hydrogen peroxide in a deoxygenated PBS at pH 7.4, as in Fig. 6a, red-brown solutions of the Mn(III)TMPyP complex in the electrochemical cell take on a dark green tint. These solutions turn brown after contact with air (oxygen) during transfer and measurement in a cuvette. Unlike the previous case, after electrochemical experiments in the presence of oxygen, as in Fig. 6b, a brown color of the solutions is directly manifested. According to the absorption spectra, Fig. 8a, this may be explained by the presence of a small amount of a green product of the chemical oxidation of the porphyrin by hydrogen

peroxide, Mn($P^{\bullet+}$), a porphyrin π-radical cation in the deoxygenated conditions with its characteristic green color [73]. The porphyrin-oxidized derivatives of the MnPs could be Mn(III)($P^{\bullet+}$) porphyrin π-radical cation corresponding to the oxidation of the porphyrin ligand or Mn(IV)P, as e.g. in eqn. (8), with a the possibility of shuttling between two formulations Mn(III)($P^{\bullet+}$) ↔ Mn(IV)P depending on various conditions [34, 35, 42, 70, 73] as well as the oxomanganyl π-radical cation O=Mn(IV)($P^{\bullet+}$) [22]. The appearance of an absorption band at about 670 nm, broadening of the 380-420 nm region, and a diminished Soret band are characteristic features of the formation of a green cation radical, Mn($P^{\bullet+}$), which can explain the presence of a green tint of the solutions after electrochemical experiments in the deoxygenated phosphate buffer at pH 7.4. The disappearance of the green tint after the solution comes into contact with air (oxygen) agrees well with a simultaneous diminishing of a characteristic band at 670 nm, which may indicate a conversion of the Mn porphyrin π-radical cation into the Mn(IV)P oxidized form, (O=)Mn(III)($P^{\bullet+}$) ↔ (O=)Mn(IV)P, after contact with oxygen in air [42, 73, 74] and further degradation products. This is in agreement with the data in [46], where O=Mn(IV)TMPyP species were formed in the presence of oxygen. Accordingly, the characteristic absorption bands of porphyrin at 462 nm and 561 nm and the absorbance at 670 nm, which are present in the deoxygenated sample, diminish progressively during the spectrophotometric measurements after contact with air (oxygen) (Fig. 8a, subsequent measurements 1 to 3). Finally, spectrum 3 (black line) is similar to the spectrum of the solution after electrochemical experiments with hydrogen peroxide in the presence of oxygen, red line 4. The formation of the smaller pi-conjugated compounds as a result of the oxidative fragmentation of the porphyrin, decomposition of the complex, and formation of brown MnO_2 can be assumed to explain other spectral details of the final spectra: increase of adsorption after 500 nm in a lower wavelength region with a band at about 340 nm [46, 75, 76].

In the case of MnTSPP and MnTCPP, smaller changes in the spectra of the solutions after electrochemical experiments were observed. These changes included lower absorption intensities at the porphyrin complex wavelengths and some increase in absorbance at the shorter wavelength at about 300 - 350 nm compared to the initial complex, Fig. 8b. Similar absorption spectra were observed for the MnTCPP complex. Accordingly, the color of the solutions did not change essentially with a slight yellow-green tint appearing after the experiments within the hydrogen peroxide concentration range used.

Thus, a chemical oxidation of Mn(III)P or its electrochemically reduced Mn(II)P form by hydrogen peroxide proceeds in parallel to the electrocatalytic electrochemical reduction of hydrogen peroxide. Moreover, optical absorption experiments confirm different mechanisms of

interactions of the MnP complexes with hydrogen peroxide in deoxygenated conditions and in the presence of oxygen with a faster degradation of the porphyrin complex in the latter system, Fig. 8. Chemical oxidative destruction of metalloporphyrin and metallophthalocyanine catalysts during the H_2O_2-mediated oxidations was also reported earlier [15, 22, 34, 43, 51].

The linear dependence of the reduction peak currents on the concentration of hydrogen peroxide for the MnTCPP and MnTSPP complexes in the presence of oxygen, Fig. 7b, retains till higher concentrations of hydrogen peroxide than for the MnTMPyP complex, whereas the reduction currents and electrochemical sensitivity to hydrogen peroxide are essentially smaller in comparison with MnTMPyP, Fig 7. This is in agreement with a stronger interaction of MnTMPyP and its electrochemically reduced metal form with hydrogen peroxide, and promotes the electrocatalytic reduction of hydrogen peroxide, but at the same time results in a faster degradation of the MnTMPyP complex, which is also in agreement with the results of the absorption experiments, Fig. 8.

Thus, based on the results of electrochemical and spectrophotometric experiments, it can be concluded that the process of hydrogen peroxide electrocatalytic reduction by the water-soluble Mn porphyrin complexes in aqueous solutions proceeds simultaneously with oxygen reduction, as well as with the homogeneous oxidation of manganese complexes by hydrogen peroxide. The presence of oxygen in a system results in higher currents but a faster degradation of the porphyrin. The results of this study also imply that in biological systems in the presence of the reducing agents which can initiate a $Mn^{III/II}P$ reduction process the formation of the reactive oxygen species (ROS), such as the superoxide anion radical and hydrogen peroxide from the oxygen reduction, and at the same time further interactions initiated by ROS should be considered simultaneously in the presence of this biomimetic catalyst.

3.4. Electrocatalytic reduction of hydrogen peroxide with Mn porphyrin complexes, pH 10.

As at pH 7.4, no wave of the Mn(III)/Mn(II) reduction is observed in the cathodic region in the presence of oxygen, Fig. 4 a,b. In the alkaline buffer solution, pH 10, the reduction of Mn(III) and O_2 is merged with a positive shift of O_2 reduction of about 0.07 V for Mn(III)MPyP and 0.01 V for Mn(III)CPP, Fig. 4 a,b. The shift is, however, smaller than in the phosphate buffer, pH 7.4. Figures 9a and S6 show examples of cyclic voltammograms of the MnP solutions in the presence of hydrogen peroxide in the deoxygenated alkaline buffer and in the presence of oxygen. A plateau of the reduction current is also observed in the deoxygenated alkaline buffer in the presence of hydrogen peroxide after the current maximum at about -0.48

V, Fig. 9a, which is similar to pH 7.4. However, it is observed at low concentrations of hydrogen peroxide and is less pronounced. Unlike pH 7.4, a two-electron reduction of the MnTMPyP complex at about -0.69 V and -0.77 V, Fig. 6 a and b, is not observed in the presence of hydrogen peroxide in the alkaline borate buffer, pH 10, Fig. 9a.

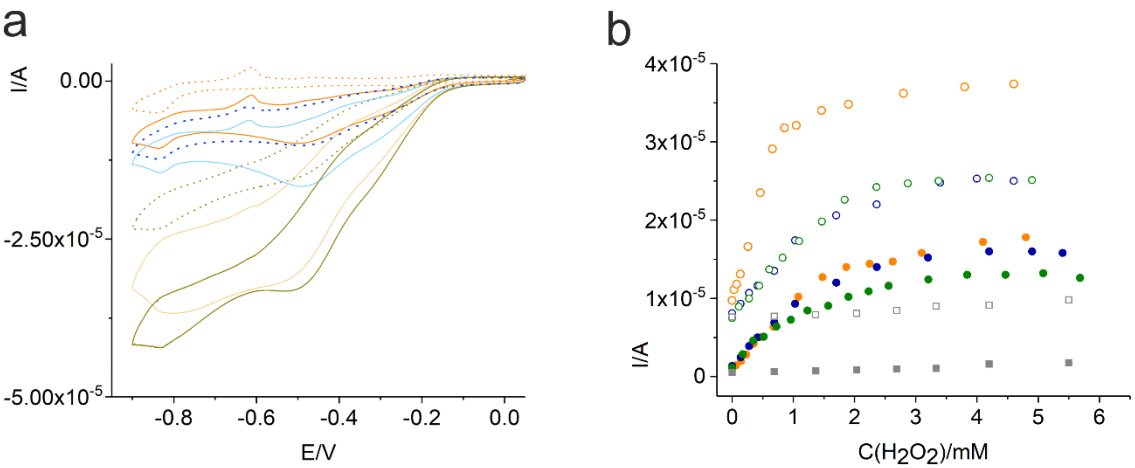

Figure 9. a. Cyclic voltammograms of the MnTMPyP complex, $9 \cdot 10^{-5}$ M, in a borate buffer solution, pH 10, *dotted lines* - in the deoxygenated buffer solutions with 0 M (orange line), $1 \cdot 10^{-3}$ M (blue line), and $2.6 \cdot 10^{-3}$ M (dark yellow line) H_2O_2, *solid lines* - in the presence of oxygen: with 0 M (orange line), $2.6 \cdot 10^{-4}$ M, $6.6 \cdot 10^{-4}$ M, and $1 \cdot 10^{-3}$ M (dark yellow line) H_2O_2; **b.** dependence of the reduction current on the concentration of hydrogen peroxide: MnTMPyP - orange circles, MnTCPP - blue circles, MnTSPP - green circles, and bare GCE - gray squares; *closed symbols* - deoxygenated solutions, *open symbols* - in the presence of oxygen, the potential values at which the reduction current values were taken for the graphs are given in Table 5.

Similar to pH 7.4, three porphyrin complexes demonstrate a higher current response to the changes of the H_2O_2 compared to that of a GCE, Fig. 9b and Table 5. However, sensitivity in the alkaline media is higher than that in pH 7.4. This indicates that $H_2O_2 \rightarrow HO_2^- + H^+$, which is more pronounced in alkaline medium, is an important intermediate step in the electrocatalytic reduction process, which was also assumed in [23] and the HO_2^- interaction with a porphyrin complex in an axial position is favorable in comparison with H_2O_2. Hence, an activating role of the hydroxide ions in accepting H^+ from an oxygen atom of hydrogen peroxide, which is coordinated to the porphyrin complex in an axial position in step (equation 7), to produce Mn-hydroperoxo (equation 7) and further Mn-oxo (equation 8) compounds may be suggested, which is similar to the role of a distal histidine in the heme peroxidase acting as a base in the

deprotonation step of H_2O_2 during the formation of compound I [69]. The coordinated hydrogen peroxide was shown to be deprotonated in this pH region [44]. Thus, in the alkaline media the electrocatalytic activity of the MnP complexes is more pronounced.

Table 5. Slope and correlation coefficients of the I-c(H_2O_2) curves at pH 10[1].

	deoxygenated[2]		in the presence of oxygen[2]	
MnTCPP	$7.7 \cdot 10^{-3}$ (E=-0.5 V)	0.9939	$8.7 \cdot 10^{-3}$ (E=-0.57 V)	0.9883
MnTSPP	$7.9 \cdot 10^{-3}$ (E=-0.5 V)	0.9305	$9.0 \cdot 10^{-3}$ (E=-0.57 V)	0.9918
MnTMPyP	$8.5 \cdot 10^{-3}$ (E=-0.48 V)	0.9956	$2.9 \cdot 10^{-2}$ (E=-0.5 V)	0.9960
GCE	$1.6 \cdot 10^{-4}$ (E=-0.5 V)	0.9987	$3.9 \cdot 10^{-4}$ (E=-0.57 V)	0.9827

[1] found from the linear portions of the curves in Fig. 9b.
[2] in brackets, potential values are given, at which reduction current values for the -I-c(H_2O_2) curves were used to evaluate the slope and R^2 parameters given in the table.

At pH 10, higher reduction currents are obtained in the aerated buffer, which is similar to pH 7.4. In the presence of oxygen, MnTMPyP demonstrates the highest electrocatalytic activity at lower potential values at both pH. The linear range of the dependence of the reduction currents on the hydrogen peroxide concentration, Fig. 9b, is essentially smaller in the alkaline medium than at pH 7.4. The linear range of the reduction currents extended up to a 10-fold excess and a 7-fold excess of the H_2O_2 concentration over the concentration of the MnTMPyP complex in the deoxygenated solution and in the presence of oxygen, respectively. For MnTCPP and MnTSPP, the linear range of the reduction currents extended up to about an 11-fold excess of the H_2O_2 concentrations.

Unlike pH 7.4, after the electrochemical experiments with hydrogen peroxide in the deoxygenated alkaline borate buffer, pH 10, the solutions of the MnTMPyP complex did not display a green tint. The absorbance at 462 nm decreased and a slight increase of the absorbance at 421 nm appeared, Fig. 10 a, which can be ascribed to the O=Mn(IV)P species [35, 46, 69, 73, 77] formed in the process of chemical oxidation of Mn(III)TMPyP or its electrochemically reduced form Mn(II)TMPyP with hydrogen peroxide, e. g., Eq. (8) .

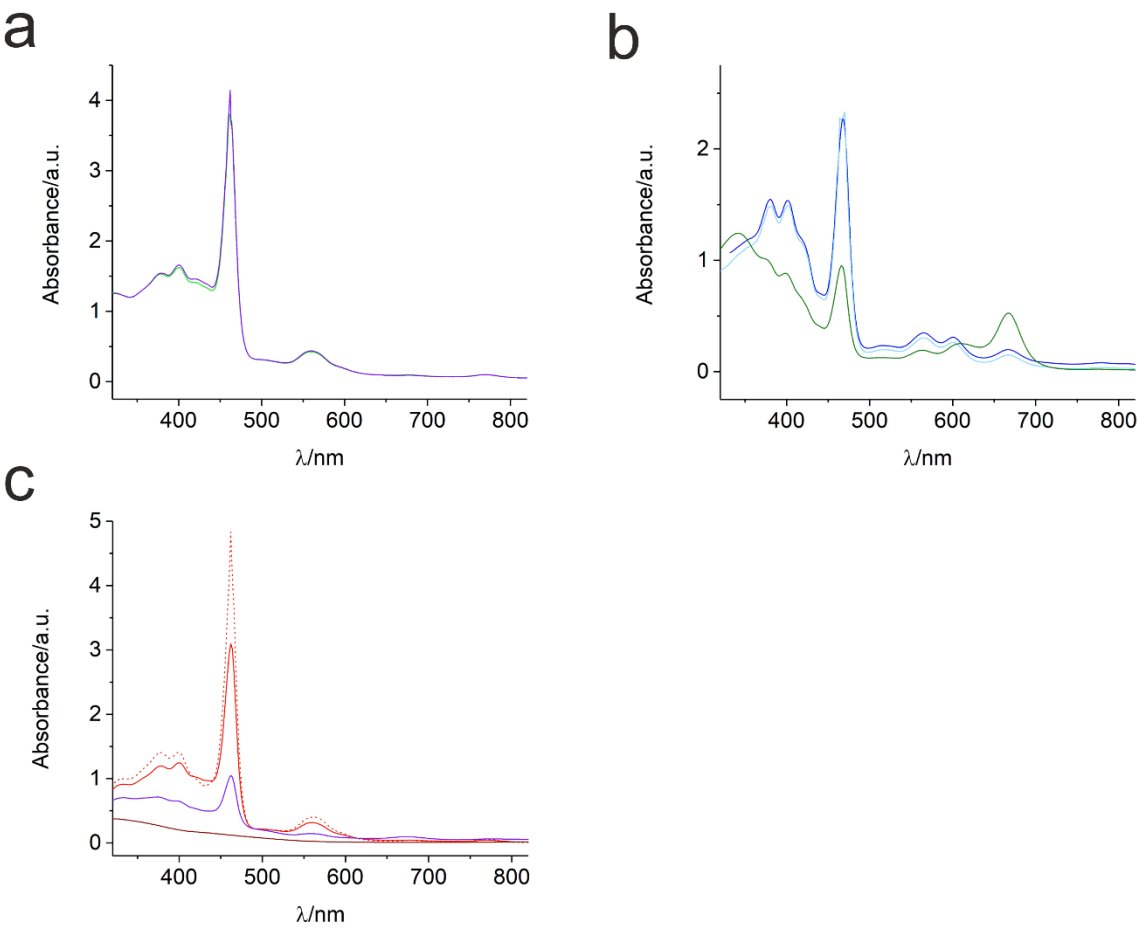

Fig. 10. Absorption spectra in borate buffer solutions, pH 10: **a.** spectrophotometric measurements of the MnTMPyP solution (initial concentration $9 \cdot 10^{-5}$ M) after electrochemical experiments in a deoxygenated buffer solution (*green line)* and in the presence of oxygen (*violet line)*; **b.** MnTCPP solution (initial concentration $9 \cdot 10^{-5}$ M) after electrochemical experiments in a deoxygenated buffer solution (diluted twice, blue line*)* and in the presence of oxygen (light blue line), and MnTSPP solution (initial concentration $9 \cdot 10^{-5}$ M) after electrochemical experiments in the presence of oxygen (green line); **c.** chemical reaction of MnTMPyP, approx. $7 \cdot 10^{-5}$ M (dotted red line), with hydrogen peroxide in the borate buffer, pH 10: $8.4 \cdot 10^{-4}$ M (solid red line) $4.6 \cdot 10^{-3}$ M (violet), 0.12 M (brown line) H_2O_2.

In contrast to MnTMPyP, the solutions of MnTCPP and MnTSPP turned intensively green, Fig. S7, during electrochemical experiments in the alkaline solutions after the concentration of hydrogen peroxide reached about $2 \cdot 10^{-3}$ M, i.e. a 22-fold excess over the concentration of the porphyrin complex. This can be explained using the data of the spectrophotometric measurements, which were recorded after the electrochemical experiments, Fig. 10 b. The spectra of the MnTCPP and MnTSPP solutions showed similar changes with a significant increase of the absorption at about 667 nm, which is characteristic of a porphyrin

ligand π-radical cation with its green color. Solutions of MnTMPyP do not exhibit this band at this concentration range of hydrogen peroxide but rather a slight increase in the region of 421 nm, which is characteristic of O=Mn(IV)P. This is in agreement with a more electronegative character of MnMPyP in comparison with MnTCPP and MnTSPP due to the electron-withdrawing properties of the N-methyl-4-pyridyl substituents in comparison with 4-sulfonatophenyl and 4-carboxyphenyl substituents, which makes a π-radical cation configuration of the oxidized MnTMPyP complex unfavorable. In this way, the main oxidation product of the MnTCPP and MnTSPP in the alkaline media in the concentration range of hydrogen peroxide studied was found to be the π-radical cation of a porphyrin ligand, while O=Mn(IV)P is observed for MnTMPyP in alkaline media.

Mn(III)TMPyP is chemically oxidized by hydrogen peroxide with a loss of the porphyrin structure by means of the higher concentrations of hydrogen peroxide with the intermediate O=Mn(IV)P (absorbance at about 425 nm, Fig. 10 c, solid red curve) and an intermediate small amount of π-radical cation (absorbance at 673 nm at a 66-fold excess of hydrogen peroxide, Fig. 10 c, violet curve). Accordingly, the π-radical cation configuration of the oxidized MnTMPyP is not favorable, which is due to the electron-withdrawing character of the N-methyl-4-pyridyl substituents of the porphyrin ring. Degradation of the metalloporphyrin catalysts in the presence of hydroxide ions or bases was also reported earlier [74].

3.5. Electrocatalytic reduction of hydrogen peroxide with Mn porphyrin complexes, pH 4.

In contrast to neutral and alkaline conditions, the cyclic voltammograms in the acidic medium, Fig. 11 a,b and S8, demonstrate reduction currents in a reverse scan direction in the same concentration ranges of hydrogen peroxide. The higher electrocatalytic reduction currents and sensitivity (slope of the $-I$ - $c(H_2O_2)$ curves), Table 6, in the case of MnTMPyP in the acidic media may be explained by the availability of protons in the media, which participate in the reduction reaction with the electrons derived from the electrode, as is schematically presented in Eqs. (1-10). In previous studies, a homolytic character of the transition state for the O-O bond cleavage was observed under basic conditions for (acylperoxo)manganese(III) porphyrin complexes, while in the protic medium the heterolytic pathways predominated [36]. The difference in the nature of the metal-mediated O-O bond dissociation in the catalytic metal-peroxide systems in alkaline and acidic media may contribute to the observed differences in the electrochemical reduction of hydrogen peroxide mediated by MnP complexes at different pH

in the present study, however, further studies are necessary to prove the intermediates of the electocatalytic reduction.

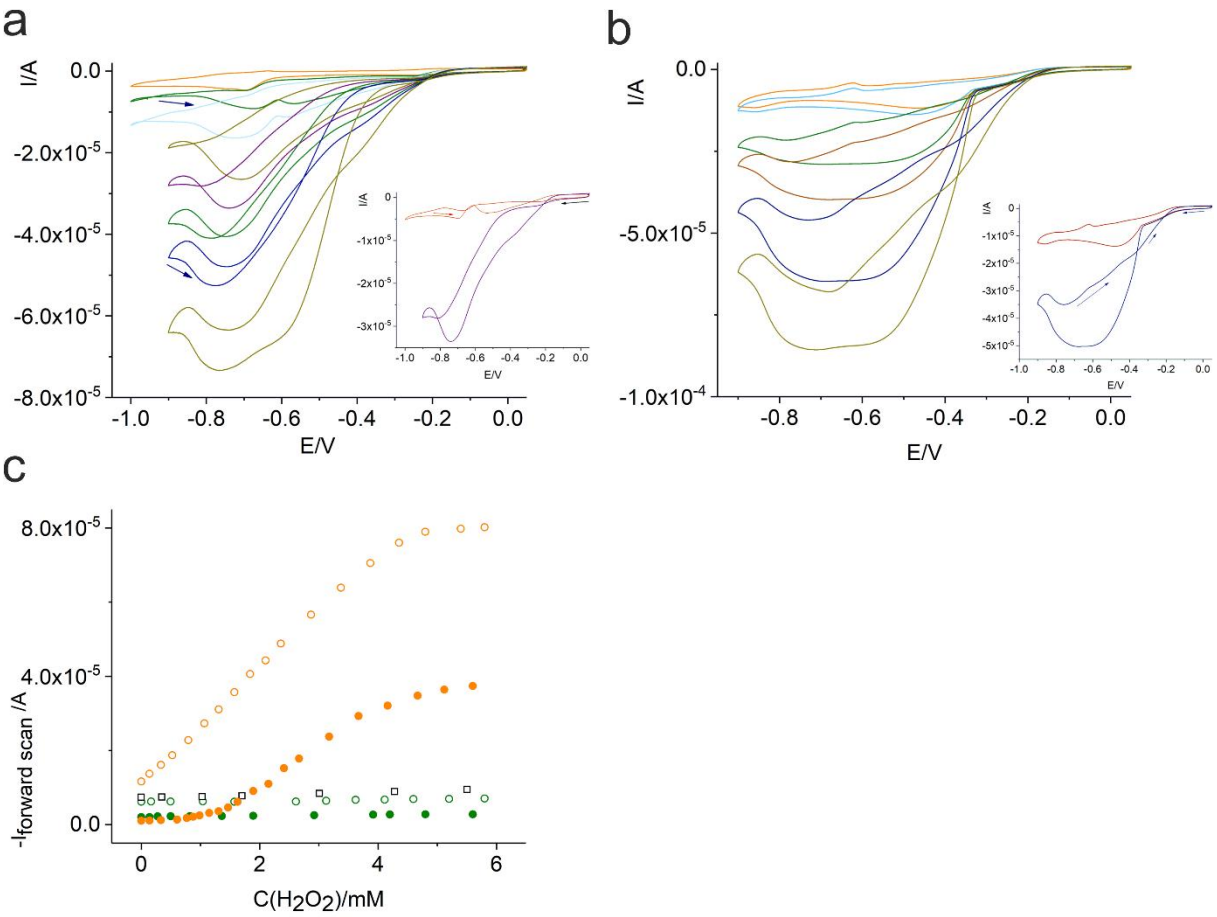

Figure 11. Cyclic voltammograms of the MnP complexes at pH 4: **a.** MnTMPyP, in the deoxygenated solution, H_2O_2 0 M (orange line), $4.2 \cdot 10^{-3}$ M (dark yellow), insert shows the CV curves at $6.1 \cdot 10^{-4}$ M and $1.6 \cdot 10^{-3}$ M H_2O_2, **b.** MnMPyP, in the presence of oxygen, H_2O_2 0 M (orange line), $4.3 \cdot 10^{-3}$ M (dark yellow line), insert shows the CV curves at $1.4 \cdot 10^{-4}$ M and $2.1 \cdot 10^{-3}$ M H_2O_2, the arrows designate the scan direction, **c.** dependences of the reduction currents in a forward scan direction on the concentration of hydrogen peroxide for MnTMPyP - orange circles (deaerated solution – solid, in the presence of oxygen - open), MnTSPP - green circles (deaerated solution – solid, in the presence of oxygen - open), GCE - open squares. Scan rate 0.05 V s^{-1}.

Table 6. Slope and correlation coefficients of the I-c(H_2O_2) curves at pH 4[1].

	deoxygenated[2]		in the presence of oxygen[2]	
MnTSPP	$1.1 \cdot 10^{-4}$ (E=-0.5 V)	0.9785	$2.5 \cdot 10^{-4}$ (E=-0.5 V)	0.8693
MnTMPyP	$1.1 \cdot 10^{-2}$ (E=-0.5 V)	0.9971	$1.6 \cdot 10^{-2}$ (E=-0.5 V)	0.9990

[1] found from the linear portions of the curves in Fig. 11c.

^{2} in brackets, potential values are given at which reduction current values for the –I - c(H_2O_2) curves were used to evaluate the slope and R^2 parameters given in the table.

In the case of MnTSPP, very low reduction currents and sensitivity, Table 6, were observed, which is similar to the reduction of hydrogen peroxide on a bare GCE, Figs. 11c and S8. Taking into account broadening of the reduction peak of the Mn(III/II)TSPP process, Fig. 5 a, in comparison with the neutral and alkaline media as well as a slight decrease in the extinction coefficient of the Mn(III)TSPP complex at 466 nm of about 1.1 times as calculated in the acidic media in comparison with pH 7.4, we can assume that this lower reactivity of the MnTSPP complex may be explained by the formation of the molecular associates due to the change of the charge balance of the porphyrin molecular tectons [78-80]. Since pK_a(-SO_3H)=4.8, sulfonic groups of the *meso*-sulfonatophenyl substituents of the porphyrin ring of the Mn(III)TSPP complex start to be protonated at pH 4, thus diminishing the net negative molecular charge. This process can result in a closer approach and association of the MnTSPP porphyrin molecules, which is often responsible for the lower extinction coefficients. At the same time, molecular association decreases the axial ligand positions available for oxygen and hydrogen peroxide reactions.

Interestingly, the color and the absorption spectra of the solutions manifested no essential changes after electrochemical experiments, Fig. 12, which implies that the porphyrin complexes were more stable at these conditions than in the neutral and alkaline media. In the neutral and alkaline media with the low concentration of hydrogen ions necessary for the reduction of oxygen and hydrogen peroxide, the porphyrin molecules could undergo oxidative fragmentation to smaller π-conjugated compounds, which absorb above 350 nm, as discussed in Sections 3.3 and 3.4, leading to the epoxidation of the C=C double bonds (similar to the epoxidation reaction with H_2O_2 catalyzed by Mn(III) complexes) [4, 27], thus inducing a faster degradation of the porphyrin catalysts to the smaller fragments, as evidenced from the absorption spectroscopy experiments. At pH 4, the hydrogen ions are more readily available from the media both for the porphyrin ligand reduction (Scheme 2) and incompletely reduced oxygen (Eqs. 1-10).

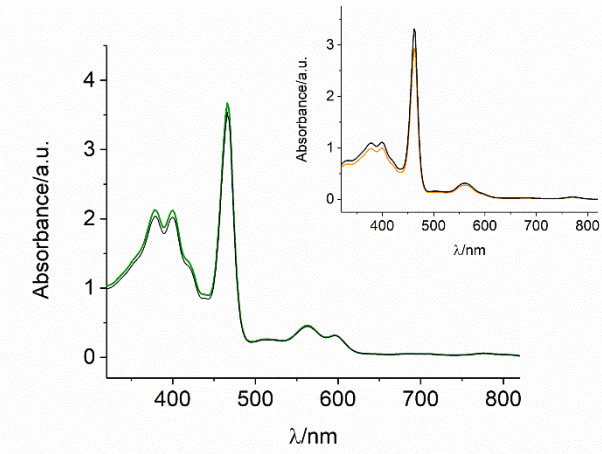

Fig. 12. Absorption spectra at pH 4: MnTSPP solution (initial concentration $9 \cdot 10^{-5}$ M) after electrochemical experiments in a deoxygenated solution (solid green line) and in the presence of oxygen (black line), insert shows the spectrophotometric measurements of the diluted MnMPyP solutions after electrochemical experiments in a deoxygenated solution (black line) and in the presence of oxygen (orange line).

Conclusion.

This paper presents the results of the study on the electrochemical properties and biomimetic activity of a series of water-soluble *meso*-substituted Mn(III) porphyrin complexes in the electrocatalytic reduction of hydrogen peroxide in aqueous solutions. MnTMPyP was most effective in the electrocatalytic reduction of hydrogen peroxide in comparison with other representative water-soluble porphyrins, MnTCPP and MnTSPP, due to the higher electron transfer constant, positive molecular charge, and the electron-withdrawing properties of its *meso*-substituents of the porphyrin macrocycle. Although electrocatalytic reduction of hydrogen peroxide was observed in all three pH regions in the deoxygenated buffer and in the presence of oxygen, a strong difference was manifested in neutral, alkaline, and acidic media. Higher electrocatalytic activity was observed in alkaline and acidic media in the presence of oxygen due to the deprotonation of hydrogen peroxide in alkaline media and the availability of hydrogen ions participating in the reduction reaction in acidic media, respectively. Mechanisms of the interactions and the intermediate products are proposed and discussed. The results of this study demonstrate that the electrochemical systems with biomimetic manganese porphyrin complexes can provide a means of electrochemically synthesizing intermediates derived from oxygen or incompletely reduced oxygen and can also be employed for the development of non-enzymatic hydrogen peroxide sensors, biomimetic (electro)catalysis, and energy research. The results also imply that in biological systems in the presence of the reducing agents which can initiate a $Mn^{III/II}P$ reduction process, formation of the reactive oxygen species such as the

superoxide anion radical and hydrogen peroxide from oxygen reduction as well as their further reaction pathways should be considered simultaneously in the presence of this biomimetic catalyst.

Supplementary Data.

Highlights

- Biomimetic properties of Mn porphyrin complexes for electrocatalytic reduction of hydrogen peroxide
- Electrogenerated reduced form of Mn porphyrins as a catalyst
- Influence of meso-substitution of the ligand macrocycle
- Different mechanisms of chemical and electrochemical reaction depending on oxygen and pH

Graphical Abstract.

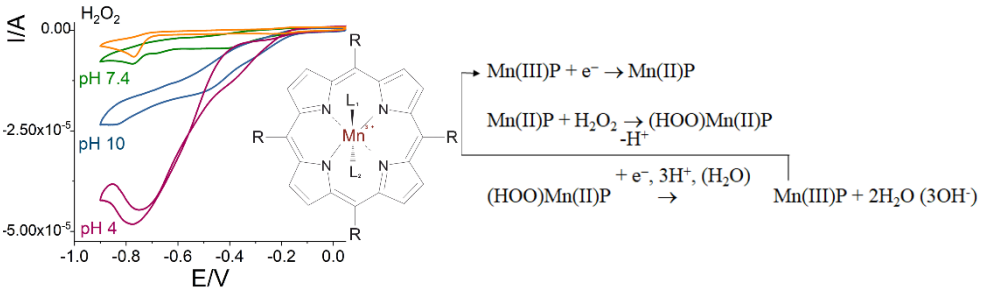

References.

[1] B. Chance, H. Sies, A. Boveris, Hydroperoxide metabolism in mammalian organs, Physiol Rev 59(3) (1979) 527-605.
[2] M. Armogida, R. Nisticò, N.B. Mercuri, Therapeutic potential of targeting hydrogen peroxide metabolism in the treatment of brain ischaemia, British Journal of Pharmacology 166(4) (2012) 1211-1224.
[3] S. Fukuzumi, Y. Yamada, K.D. Karlin, Hydrogen peroxide as a sustainable energy carrier: Electrocatalytic production of hydrogen peroxide and the fuel cell, Electrochimica Acta 82 (2012) 493-511.
[4] O.Y. Lyakin, R.V. Ottenbacher, K.P. Bryliakov, E.P. Talsi, Asymmetric epoxidations with H2O2 on Fe and Mn aminopyridine catalysts: probing the nature of active species by combined electron paramagnetic resonance and enantioselectivity study, ACS Catalysis 2(6) (2012) 1196-1202.
[5] M. Oszajca, A. Franke, M. Brindell, G. Stochel, R. van Eldik, Redox cycling in the activation of peroxides by iron porphyrin and manganese complexes. 'Catching' catalytic active intermediates, Coordination Chemistry Reviews 306 (2016) 483-509.
[6] S.M. Adam, G.B. Wijeratne, P.J. Rogler, D.E. Diaz, D.A. Quist, J.J. Liu, K.D. Karlin, Synthetic Fe/Cu complexes: toward understanding Heme-Copper Oxidase structure and function, Chemical Reviews 118(22) (2018) 10840-11022.
[7] R.A. Baglia, J.P.T. Zaragoza, D.P. Goldberg, Biomimetic reactivity of oxygen-derived manganese and iron porphyrinoid complexes, Chemical Reviews 117(21) (2017) 13320-13352.
[8] Q. He, Mugadza, Hwang, T. Nyokong, Mechanisms of Electrocatalysis of oxygen reduction by metal porphrins in trifluoromethane sulfonic acid solution, Int. J. Electrochem. Sci. 8 (2012) 7045-7064.

[9] J.H. Zagal, S. Griveau, J.F. Silva, T. Nyokong, F. Bedioui, Metallophthalocyanine-based molecular materials as catalysts for electrochemical reactions, Coordination Chemistry Reviews 254(23) (2010) 2755-2791.
[10] D. Fapyane, L. Kékedy-Nagy, I.Y. Sakharov, E.E. Ferapontova, Electrochemistry and electrocatalysis of covalent hemin-G4 complexes on gold, Journal of Electroanalytical Chemistry 812 (2018) 174-179.
[11] Y. Shu, J. Chen, Z. Xu, D. Jin, Q. Xu, X. Hu, Nickel metal-organic framework nanosheet/hemin composite as biomimetic peroxidase for electrocatalytic reduction of H2O2, Journal of Electroanalytical Chemistry 845 (2019) 137-143.
[12] K. Amreen, A.S. Kumar, A human whole blood chemically modified electrode for the hydrogen peroxide reduction and sensing: Real-time interaction studies of hemoglobin in the red blood cell with hydrogen peroxide, Journal of Electroanalytical Chemistry 815 (2018) 189-197.
[13] P.A. Forshey, T. Kuwana, Electrochemistry of oxygen reduction. 4. Oxygen to water conversion by iron(II)(tetrakis(N-methyl-4-pyridyl)porphyrin) via hydrogen peroxide, Inorganic Chemistry 22(5) (1983) 699-707.
[14] W. Chen, W. Weng, X. Niu, X. Li, Y. Men, W. Sun, G. Li, L. Dong, Boron-doped Graphene quantum dots modified electrode for electrochemistry and electrocatalysis of hemoglobin, Journal of Electroanalytical Chemistry 823 (2018) 137-145.
[15] C.F. Kolpin, H.S. Swofford, Heme catalyzed reduction of oxygen and hydrogen peroxide at a mercury electrode surface, Analytical Chemistry 50(7) (1978) 920-929.
[16] J. Masa, K. Ozoemena, W. Schuhmann, J.H. Zagal, Oxygen reduction reaction using N4-metallomacrocyclic catalysts: fundamentals on rational catalyst design, Journal of Porphyrins and Phthalocyanines 16(07n08) (2012) 761-784.
[17] D. den Boer, M. Li, T. Habets, P. Iavicoli, A.E. Rowan, R.J.M. Nolte, S. Speller, D.B. Amabilino, S. De Feyter, J.A.A.W. Elemans, Detection of different oxidation states of individual manganese porphyrins during their reaction with oxygen at a solid/liquid interface, Nature Chemistry 5 (2013) 621.
[18] C.M. Maroneze, Y. Gushikem, L.T. Kubota, Applications of MN4 Macrocyclic Metal Complexes in Electroanalysis, in: J. Zagal, F. Bedioui (Eds.), Electrochemistry of N4 Macrocyclic Metal Complexes, Springer, Switzerland, 2016.
[19] B. Sun, Z. Ou, S. Yang, D. Meng, G. Lu, Y. Fang, K.M. Kadish, Synthesis and electrochemistry of β-pyrrole nitro-substituted cobalt(ii) porphyrins. The effect of the NO2 group on redox potentials, the electron transfer mechanism and catalytic reduction of molecular oxygen in acidic media, Dalton Transactions 43(28) (2014) 10809-10815.
[20] Y.O. Su, T. Kuwana, S.-M. Chen, Electrocatalysis of oxygen reduction by water-soluble iron porphyrins: Thermodynamic and kinetic advantage studies, Journal of Electroanalytical Chemistry and Interfacial Electrochemistry 288(1) (1990) 177-195.
[21] I. Batinić-Haberle, J.S. Rebouças, I. Spasojević, Superoxide dismutase mimics: chemistry, pharmacology, and therapeutic potential, Antioxid Redox Signal 13(6) (2010) 877-918.
[22] L. Leone, D. D'Alonzo, V. Balland, G. Zambrano, M. Chino, F. Nastri, O. Maglio, V. Pavone, A. Lombardi, Mn-Mimochrome VI*a: An Artificial Metalloenzyme With Peroxygenase Activity, Frontiers in Chemistry 6(590) (2018).
[23] D.A. Stoyanovsky, Z. Huang, J. Jiang, N.A. Belikova, V. Tyurin, M.W. Epperly, J.S. Greenberger, H. Bayir, V.E. Kagan, A manganese–porphyrin complex decomposes H2O2, inhibits apoptosis, and acts as a radiation mitigator in vivo, ACS Medicinal Chemistry Letters 2(11) (2011) 814-817.
[24] M. Chino, L. Leone, G. Zambrano, F. Pirro, D. D'Alonzo, V. Firpo, D. Aref, L. Lista, O. Maglio, F. Nastri, A. Lombardi, Oxidation catalysis by iron and manganese porphyrins within enzyme-like cages, Biopolymers 109(10) (2018) e23107.
[25] I. Batinić-Haberle, I. Spasojević, R.D. Stevens, P. Hambright, I. Fridovich, Manganese(III) *meso*-tetrakis(ortho-N-alkylpyridyl)porphyrins. Synthesis, characterization, and catalysis of $O_2^{\cdot -}$ dismutation, Journal of the Chemical Society, Dalton Transactions (13) (2002) 2689-2696.

[26] A. Prasad, A. Kumar, M. Suzuki, H. Kikuchi, T. Sugai, M. Kobayashi, P. Pospíšil, M. Tada, S. Kasai, Detection of hydrogen peroxide in Photosystem II (PSII) using catalytic amperometric biosensor, Frontiers in Plant Science 6(862) (2015).
[27] J.C. Barona-Castaño, C.C. Carmona-Vargas, T.J. Brocksom, K.T. De Oliveira, Porphyrins as catalysts in scalable organic reactions, Molecules 21 (2016) 310.
[28] S. Aime, M. Botta, E. Gianolio, E. Terreno, A p(O2)-responsive MRI contrast agent based on the redox switch of manganese(II / III) – porphyrin complexes, Angewandte Chemie International Edition 39(4) (2000) 747-750.
[29] E. Koposova, G. Shumilova, Y. Ermolenko, A. Kisner, A. Offenhaeusser, Y. Mourzina, Direct electrochemistry of cyt c and hydrogen peroxide biosensing on oleylamine- and citrate-stabilized gold nanostructures, Sensors and Actuators B-Chemical 207 (2015) 1045-1052.
[30] R. Paolesse, S. Nardis, D. Monti, M. Stefanelli, C. Di Natale, Porphyrinoids for Chemical Sensor Applications, Chemical Reviews 117(4) (2017) 2517-2583.
[31] T.A. Skripnikova, A.A. Starikova, G.I. Shumilova, Y.E. Ermolenko, A.A. Pendin, Y.G. Mourzina, Towards stabilization of the potential response of Mn(III) tetraphenylporphyrin-based solid-state electrodes with selectivity for salicylate ions, Journal of Solid State Electrochemistry 21(8) (2017) 2269-2279.
[32] S. Fukuzumi, H. Imahori, Biomimetic electron-transfer chemistry of porphyrins and metalloporphyrins, in: V. Balzani (Ed.), Electron Transfer in Chemistry, Wiley-VCH, Weinheim, Germany, 2001, pp. 927-975.
[33] E. Koposova, X. Liu, A. Pendin, B. Thiele, G. Shumilova, Y. Ermolenko, A. Offenhäusser, Y. Mourzina, Influence of Meso-Substitution of the Porphyrin Ring on Enhanced Hydrogen Evolution in a Photochemical System, The Journal of Physical Chemistry C 120(26) (2016) 13873-13890.
[34] T.N. Lomova, M.V. Klyuev, E.N. Ovchenkova, M.E. Klyueva, Kinetics and mechanism of decomposition of hydrogen peroxide in the presence of manganese(III) porphyrins, Russian Journal of General Chemistry 80(5) (2010) 1011-1017.
[35] R.S. Czernuszewicz, Y.O. Su, M.K. Stern, K.A. Macor, D. Kim, J.T. Groves, T.G. Spiro, Oxomanganese(IV) porphyrins identified by resonance Raman and infrared spectroscopy. Weak bonds and the stability of the half-filled t2g subshell, Journal of the American Chemical Society 110(13) (1988) 4158-4165.
[36] J.T. Groves, Y. Watanabe, Heterolytic and homolytic oxygen-oxygen bond cleavage reactions of acylperoxomanganese(III) porphyrins, Inorganic Chemistry 25(27) (1986) 4808-4810.
[37] Y. Naruta, K. Maruyama, High oxygen-evolving activity of rigidly linked manganese(III) porphyrin dimers. A functional model of manganese catalase, Journal of the American Chemical Society 113(9) (1991) 3595-3596.
[38] L. Wang, Y. Fang, J. Xu, Z. Ou, K.M. Kadish, Electrochemical and spectroelectrochemical characterization of Cu(II) and Mn(III) tetrabutano- and tetrabenzoporphyrins containing sterically hindered meso -(2,6-difluorophenyl) substituents in nonaqueous media, Journal of Porphyrins and Phthalocyanines 23(09) (2019) 1057-1071.
[39] B.E. Murphy, S.A. Krasnikov, N.N. Sergeeva, A.A. Cafolla, A.B. Preobrajenski, A.N. Chaika, O. Lübben, I.V. Shvets, Homolytic Cleavage of Molecular Oxygen by Manganese Porphyrins Supported on Ag(111), ACS Nano 8(5) (2014) 5190-5198.
[40] M.I. Bazanov, A.V. Petrov, G.V. Zhutaeva, I.V. Turchaninova, G. Andrievski, A.A. Evseev, Electrocatalytic activity of macroheterocyclic complexes in the molecular oxygen electroreduction: A cyclic voltammetry estimate, Russian Journal of Electrochemistry 40(11) (2004) 1198-1204.
[41] N.M. Berezina, M.E. Klueva, M.I. Bazanov, Electrochemical characterization of β-alkyl substituted porphyrins and Mn(III) complexes in alkaline solution, Macroheterocycles 10(3) (2017) 308-312.
[42] N. Carnieri, A. Harriman, G. Porter, Photochemistry of manganese porphyrins. Part 6. Oxidation–reduction equilibria of manganese(III) porphyrins in aqueous solution, Journal of the Chemical Society, Dalton Transactions (5) (1982) 931-938.
[43] D.V. Konev, O.I. Istakova, B. Dembinska, M. Skunik-Nuckowska, C.H. Devillers, O. Heintz, P.J. Kulesza, M.A. Vorotyntsev, Electrocatalytic properties of manganese and cobalt polyporphine films toward oxygen reduction reaction, Journal of Electroanalytical Chemistry 816 (2018) 83-91.

[44] N. Jin, D.E. Lahaye, J.T. Groves, A “Push−Pull” Mechanism for Heterolytic O−O Bond Cleavage in Hydroperoxo Manganese Porphyrins, Inorganic Chemistry 49(24) (2010) 11516-11524.
[45] N. Kobayashi, H. Saiki, T. Osa, Catalytic electroreduction of molecular oxygen using [5,10,15,20-tetrakis-(1-methylpyridinium-4-yl)porphinato]manganese, Chemistry Letters 14(12) (1985) 1917-1920.
[46] O. Ramirez-Gutierrez, J. Claret, J.M. Ribo, Oxidation states of manganese porphyrins in water solutions, J. Porphyrins Phthalocyanines 9 (2005) 436-443.
[47] T. Weitner, I. Kos, Z. Mandić, I. Batinić-Haberle, M. Biruš, Acid–base and electrochemical properties of manganese meso(ortho- and meta-N-ethylpyridyl)porphyrins: voltammetric and chronocoulometric study of protolytic and redox equilibria, Dalton Transactions 42(41) (2013) 14757-14765.
[48] F.-c. Chen, S.-H. Cheng, C.-H. Yu, M.-H. Liu, Y.O. Su, Electrochemical characterization and electrocatalysis of high valent manganese meso-tetrakis(N-methyl-2-pyridyl)porphyrin, Journal of Electroanalytical Chemistry 474(1) (1999) 52-59.
[49] F. De Angelis, N. Jin, R. Car, J.T. Groves, Electronic Structure and Reactivity of Isomeric Oxo-Mn(V) Porphyrins: Effects of Spin-State Crossing and pKa Modulation, Inorganic Chemistry 45(10) (2006) 4268-4276.
[50] C.-Y. Lin, Z.-F. Lin, T.-M. Hseu, Y. Oliver Su, Speciation, catalysis and transmetallation of manganese tetrakls(N-methyl-4-pyridyl)porphine in aqueous media, Journal of the Chinese Chemical Society 37(4) (1990) 335-344.
[51] T.N. Lomova, E.N. Kiseleva, M.E. Klyueva, Kinetics and mechanism of oxidation of manganese(III) acidoporphyrin complexes with hydrogen peroxide, Russian Journal of Inorganic Chemistry 51(11) (2006) 1820-1825.
[52] F. Schröper, D. Brüggemann, Y. Mourzina, B. Wolfrum, A. Offenhäusser, D. Mayer, Analyzing the electroactive surface of gold nanopillars by electrochemical methods for electrode miniaturization, Electrochimica Acta 53(21) (2008) 6265-6272.
[53] J.M. McCord, I. Fridovich, Superoxide Dismutase: an enzymatic function for erythrocuprein (hemocuprein), Journal of Biological Chemistry 244(22) (1969) 6049-6055.
[54] Y. Sawada, I. Yamazaki, One-electron transfer reactions in biochemical systems. VII. Kinetic study of superoxide dismutase., Biochimica et Biophysica Acta 327 (1973) 257-265.
[55] K.M. Faulkner, S.I. Liochev, I. Fridovich, Stable Mn(III) Porphyrins mimic superoxide dismutase in vitro and substitute for it in vivo., The Journal of Biological Chemistry 269(38) (1994) 23471-23476.
[56] I. Spasojević, I. Batinić-Haberle, R.D. Stevens, P. Hambright, A.N. Thorpe, J. Grodkowski, P. Neta, I. Fridovich, Manganese(III) Biliverdin IX Dimethyl Ester: A Powerful Catalytic Scavenger of Superoxide Employing the Mn(III)/Mn(IV) Redox Couple, Inorganic Chemistry 40(4) (2001) 726-739.
[57] O. Horváth, Z. Valicsek, G. Harrach, G. Lendvay, M.A. Fodor, Spectroscopic and photochemical properties of water-soluble metalloporphyrins of distorted structure, Coordination Chemistry Reviews 256(15) (2012) 1531-1545.
[58] K. Takahashi, T. Komura, H. Imanaga, Light-induced Redox Characteristics of [Tetrakis(4-methylpyridyl)porphyrinato]manganese(III), Bulletin of the Chemical Society of Japan 56(11) (1983) 3203-3207.
[59] L.J. Boucher, Manganese porphyrin complexes, Coordination Chemistry Reviews 7(3) (1972) 289-329.
[60] M. Jahan, Q. Bao, K.P. Loh, Electrocatalytically Active Graphene–Porphyrin MOF Composite for Oxygen Reduction Reaction, Journal of the American Chemical Society 134(15) (2012) 6707-6713.
[61] A. Harriman, Photochemistry of manganese porphyrins. Part 8. Electrochemistry, Journal of the Chemical Society, Dalton Transactions (2) (1984) 141-146.
[62] R.S. Nicholson, Theory and application of cyclic voltammetry for measurement of electrode reaction kinetics. , Analytical Chemistry 37(11) (1965) 1351-1355.
[63] V.G. Mairanovsky, Electrochemistry of porphyrins, in: N.S. Enikolopian (Ed.), Porphyrins: spectrosopy, electrochemistry, application, Nauka, Moscow, 1987, pp. 127-178.
[64] L. Cong, M.K. Chahal, R. Osterloh, M. Sankar, K.M. Kadish, Synthesis, electrochemistry, and reversible interconversion among perhalogenated hydroxyphenyl Ni(II) porphyrins,

porphodimethenes, and porpho-5,15-bis-paraquinone methide, Inorganic Chemistry 58(21) (2019) 14361-14376.
[65] M.L. Pegis, C.F. Wise, D.J. Martin, J.M. Mayer, Oxygen reduction by homogeneous molecular catalysts and electrocatalysts, Chemical Reviews 118(5) (2018) 2340-2391.
[66] W. Zhang, W. Lai, R. Cao, Energy-related small molecule activation reactions: oxygen reduction and hydrogen and oxygen evolution reactions catalyzed by porphyrin- and corrole-based systems, Chemical Reviews 117(4) (2017) 3717-3797.
[67] R. Cao, C. Saracini, J.W. Ginsbach, M.T. Kieber-Emmons, M.A. Siegler, E.I. Solomon, S. Fukuzumi, K.D. Karlin, Peroxo and superoxo moieties bound to copper ion: electron-transfer equilibrium with a small reorganization energy, Journal of the American Chemical Society 138(22) (2016) 7055-7066.
[68] M.E. Lai, A. Bergel, Electrochemical reduction of oxygen on glassy carbon: catalysis by catalase, Journal of Electroanalytical Chemistry 494(1) (2000) 30-40.
[69] B. Meunier, J. Bernadou, Active iron-oxo and iron-peroxo species incytochromes P450 and peroxidases, in: B. Meunier (Ed.), Structure and bonding, Springer, Berlin-Heidelberg, 2000, pp. 1-36.
[70] T.N. Lomova, M.E. Klyueva, M.V. Klyuev, The mechanism of catalytic action of the coordination centres of catalase synthetic models, in: T.N. Lomova, G. Zaikov (Eds.), Chemical Processes with Participation of Biological and Related Compounds: Biophysical and Chemical Aspects of Porphyrins, Pigments, Drugs, Biodegradable Polymers and Nanofibers, CRC Press2008, pp. 93-116.
[71] M. Procner, L. Orzel, G. Stochel, R. van Eldik, Spectroscopic and kinetic evidence for redox cycling, catalase and degradation activities of Mn(III)(TPPS) in a basic aqueous peroxide medium, Chem Commun (Camb) 52(30) (2016) 5297-300.
[72] R. Kubota, S. Imamura, T. Shimizu, S. Asayama, H. Kawakami, Synthesis of water-soluble dinuclear mn-porphyrin with multiple antioxidative activities, ACS Med Chem Lett 5(6) (2014) 639-43.
[73] L. Kaustov, M.E. Tal, A.I. Shames, Z. Gross, Spin transition in a manganese(III) porphyrin cation radical, its transformation to a dichloromanganese(IV) porphyrin, and chlorination of hydrocarbons by the latter, Inorganic Chemistry 36(16) (1997) 3503-3511.
[74] T.N. Lomova, M.V. Klyuev, M.E. Klyueva, E.N. Kiseleva, O.V. Kosareva, Substituted porphyrins in bioinorganic chemistry., Journal of Russian Chemical Society D. I. Mendeleev 48 (2004) 35-51.
[75] C.N. Butterfield, A.V. Soldatova, S.-W. Lee, T.G. Spiro, B.M. Tebo, Mn(II,III) oxidation and MnO₂ mineralization by an expressed bacterial multicopper oxidase, Proceedings of the National Academy of Sciences 110(29) (2013) 11731-11735.
[76] N. Sakai, Y. Ebina, K. Takada, T. Sasaki, Electrochromic films composed of MnO2 nanosheets with controlled optical density and high coloration efficiency, J Electrochem Soc 152(12) (2005) E384-E389.
[77] H. Volz, W. Müller, Isolation and characterization of a porphinatomanganese(IV) complex from the reaction of dichloro monoxide with 5,10,15,20-tetrakis-(2,6-dichloropheny)porphinatomanganese(III) chloride [Mn(EDCPP)CI], Chemische Berichte 130(8) (1997) 1099-1103.
[78] E.A. Koposova, Y.E. Ermolenko, A. Offenhausser, Y.G. Mourzina, Self-assembly and photoconductivity of binary porphyrin nanostructures of meso-tetrakis(4-sulfonatophenyl)porphine and Co(III) meso-tetra(4-pyridyl)porphine chloride, Colloids and Surfaces a-Physicochemical and Engineering Aspects 548 (2018) 172-178.
[79] E.A. Koposova, A. Offenhäusser, Y.E. Ermolenko, Y.G. Mourzina, Photoresponsive porphyrin nanotubes of meso-tetra(4-sulfonatophenyl)porphyrin and Sn(IV) meso-tetra(4-pyridyl)porphyrin, Frontiers in Chemistry 7(351) (2019).
[80] E.A. Koposova, A.A. Pendin, Y.E. Ermolenko, G.I. Shumilova, A.A. Starikova, Y.G. Mourzina, Morphological properties and photoconductivity of self-assembled Sn/Co porphyrin nanostructures, Reviews on Advanced Materials Science 45(1-2) (2016) 15-19.